

METHOD

Linking aerial hyperspectral data to canopy tree biodiversity: An examination of the spectral variation hypothesis

Anna L. Crofts¹  | Christine I. B. Wallis¹  | Sabine St-Jean¹  |
 Sabrina Demers-Thibeault² | Deep Inamdar³  | J. Pablo Arroyo-Mora⁴  |
 Margaret Kalacska³  | Etienne Laliberté²  | Mark Vellend¹ 

¹Département de biologie, Université de Sherbrooke, Sherbrooke, Québec, Canada

²Département de sciences biologiques, Institut de recherche en biologie végétale, Université de Montréal, Montréal, Québec, Canada

³Department of Geography, McGill University, Montréal, Québec, Canada

⁴National Research Council of Canada, Flight Research Lab, Ottawa, Ontario, Canada

Correspondence

Anna L. Crofts
 Email: croftsanna@gmail.com

Funding information

Natural Sciences and Engineering Research Council of Canada, Grant/Award Numbers: 509190-2017, 53495-2019; Royal Canadian Geographical Society

Handling Editor: Jesús Pinto-Ledezma

Abstract

Imaging spectroscopy is emerging as a leading remote sensing method for quantifying plant biodiversity. The spectral variation hypothesis predicts that variation in plant hyperspectral reflectance is related to variation in taxonomic and functional identity. While most studies report some correlation between spectral and field-based (i.e., taxonomic and functional) expressions of biodiversity, the observed strength of association is highly variable, and the utility in applying spectral community properties to examine environmental drivers of communities remains unknown. We linked hyperspectral data acquired by airborne imaging spectrometers with precisely geolocated field plots to examine the spectral variation hypothesis along a temperate-to-boreal forest gradient in southern Québec, Canada. First, we examine the degree of association between spectral and field-based dimensions of canopy tree composition and diversity. Second, we ask whether the relationships between field-based community properties and the environment are reproduced when using spectral community properties. We found support for the spectral variation hypothesis with the strength of association generally greater for the functional than taxonomic dimension, but the strength of relationships was highly variable and dependent on the choice of method or metric used to quantify spectral and field-based community properties. Using a multivariate approach (comparisons of separate ordinations), spectral composition was moderately well correlated with field-based composition; however, the degree of association increased when univariately relating the main axes of compositional variation. Spectral diversity was most tightly associated with functional diversity metrics that quantify functional richness and divergence. For predicting canopy tree composition and diversity using environmental variables, the same qualitative conclusions emerge when hyperspectral or field-based data are used. Spatial patterns of canopy tree community properties were strongly related to the

This is an open access article under the terms of the [Creative Commons Attribution](https://creativecommons.org/licenses/by/4.0/) License, which permits use, distribution and reproduction in any medium, provided the original work is properly cited.

© 2024 The Authors. *Ecological Monographs* published by Wiley Periodicals LLC on behalf of The Ecological Society of America.

turnover from temperate-to-boreal communities, with most variation explained by elevation. Spectral composition and diversity provide a straightforward way to quantify plant biodiversity across large spatial extents without the need for a priori field observations. While commonly framed as a potential tool for biodiversity monitoring, we show that spectral community properties can be applied more widely to assess the environmental drivers of biodiversity, thereby helping to advance our understanding of the drivers of biogeographical patterns of plant communities.

KEYWORDS

biodiversity, boreal forest, hyperspectral reflectance, imaging spectroscopy, northern temperate forest, spectral composition, spectral diversity, spectral variation hypothesis

INTRODUCTION

Plants absorb and scatter light in unique and complex ways depending on their chemical and physical properties; thus, plant–light interactions provide a window through which to study plant form and function (Cavender-Bares et al., 2017; Kothari & Schweiger, 2022; Ustin & Gamon, 2010). Plants interact with sunlight across the wavelengths of incident radiation, but this interaction is only noticeable to the human eye in the visible region (400–700 nm), where leaf pigments absorb light (Jacquemoud & Baret, 1990; Ustin et al., 2009). At longer near-infrared (NIR) wavelengths (700–1100 nm), reflectance is high and the structural characteristics of leaves (e.g., intercellular spaces, cell wall thickness) and crown architecture (e.g., branching structure, leaf angle distribution) influence light scattering (Jacquemoud & Baret, 1990; Ollinger, 2011; Ustin et al., 2009). Other leaf biochemicals, including lignin, cellulose, and phenolics, have absorption features in the shortwave infrared (SWIR) region (1100–2400 nm). Imaging spectroscopy, a passive optical remote sensing approach also referred to as hyperspectral imaging, quantifies how Earth's surface materials—including vegetation—reflect light across hundreds of contiguous, narrow wavelength bands. Given that traits drive plant–light interactions, hyperspectral reflectance profiles acquired over plant canopies are increasingly considered an integrative measure of plant phenotypes (Cavender-Bares et al., 2017; Kothari & Schweiger, 2022; Ustin & Gamon, 2010).

There is great interest in applying imaging spectroscopy to better understand patterns in plant biodiversity and to monitor global change impacts, as remotely sensed data overcomes the inherent sparseness of field-based biodiversity inventories and provide spatially continuous data across the extent of the imaged area (Turner, 2014; Wang & Gamon, 2019). The spatial

resolution of imagery dictates the ecological level to which hyperspectral reflectance should relate, where at fine spatial resolutions hyperspectral data should provide information on individual plants. Centered on the premise that hyperspectral reflectance profiles are integrated measures of plant phenotypes, the spectral variation hypothesis (SVH) predicts that variation in hyperspectral reflectance within a given area (i.e., spectral diversity) should be a direct expression of plant biodiversity in the same area (originally formulated by Palmer et al. [2002] but updated by Ustin & Gamon [2010]). While the SVH explicitly predicts a direct link between spectral and field-based diversity, building off its central premise, the SVH can be extended to other properties that characterize the plant community within a given area. However, to date, uncertainty has surrounded the generality of the link between spectral and field-based community properties (Fassnacht et al., 2022).

Biodiversity is a multidimensional concept—encompassing variation in species' identities, functions, and other elements of variation of life on Earth (Purvis & Hector, 2000). While plant communities are most commonly examined at the taxonomic level (i.e., counting species and estimating their abundances), incorporating functional attributes (i.e., trait values) of organisms has greatly advanced the understanding of distributions along environmental gradients (e.g., Grime, 1979; Westoby et al., 2002), community assembly (e.g., McGill et al., 2006; Shipley, 2010), and the effects of organisms on ecosystem properties (e.g., Funk et al., 2017; Lavorel & Garnier, 2002). Given that plant traits dictate plant–light interactions, the association between spectral and taxonomic community properties is indirect, via traits (Fassnacht et al., 2022). We thus predict that support for the SVH should be stronger when predicting the functional dimension, particularly when the measured traits are causally associated with hyperspectral reflectance profiles.

For all biodiversity dimensions, a multitude of measurement methods and metrics have been proposed (Magurran & McGill, 2010; Purvis & Hector, 2000; Wang & Gamon, 2019). We are generally interested in two main community properties: composition and diversity (Magurran & McGill, 2010). Composition—which species or what trait values are present within a given area—is multivariate (i.e., vectors of species abundances or community-weighted mean trait values) and ordination methods are often used to reduce the dimensionality of composition data (Legendre & Legendre, 2012). In contrast, diversity—the variability of species abundances or trait values within a given area—is univariate and is quantified by metrics (i.e., mathematical functions) that synthesize and summarize variation in compositional data (Daly et al., 2018; Magurran & McGill, 2010; Purvis & Hector, 2000). There is no single correct way to quantify diversity, as is evident from the vast number of metrics found in the literature, where the various metrics emphasize different components of diversity: richness, evenness, and divergence (Magurran & McGill, 2010; Purvis & Hector, 2000).

The concept of composition and diversity can be extended to the spectral dimension (i.e., quantified using hyperspectral data). In an analogous manner, spectral composition is multivariate and defined by the full set of reflectance values that are present within a given area (also referred to as spectral identity; Kothari & Schweiger, 2022). Just as functional composition is quantified using community-level trait averages, spectral composition can be quantified using community-level average reflectance (Schweiger & Laliberté, 2022; Wallis et al., 2023; alternatively quantified using spectral species abundances; see Féret & Asner, 2014). Spectral diversity, correspondingly, is related to variability and quantified by metrics that summarize the variation in reflectance values within a given area (as reviewed by Wang & Gamon, 2019). Several spectral diversity metrics have been proposed to date (e.g., Dahlin, 2016; Laliberté et al., 2020; Wang et al., 2016; as reviewed by Wang & Gamon, 2019); however, less attention has been devoted to spectral composition (but see Laliberté et al., 2020; Rocchini et al., 2018; Schweiger & Laliberté, 2022). Support for the SVH is likely dependent on the choice of spectral community property and the field-based community property to which it is compared, but few studies have tested the many combination methods and metrics used to characterize communities.

The SVH has been tested using fine-resolution hyperspectral data in a variety of ecosystems, including temperate grasslands (Gholizadeh et al., 2019; Wang, Gamon, Cavender-Bares, et al., 2018), tropical forests (Draper et al., 2019; Féret & Asner, 2014), and temperate

forests (Kamoske et al., 2022) (see Rocchini et al., 2010; Schmidlein & Fassnacht, 2017; Wang & Gamon, 2019 for reviews). To date, most studies have related spectral diversity to taxonomic diversity, particularly species richness, while less attention has been paid to functional diversity (but see Kamoske et al., 2022; Schweiger et al., 2018). Moreover, the SVH has rarely been extended to examine the degree of association between spectral and field-based composition (but see Draper et al., 2019; Féret & Asner, 2014; Hakkenberg, Peet, et al., 2018; Schweiger & Laliberté, 2022; Wallis et al., 2023). The strength of support for the SVH has varied greatly across studies (Fassnacht et al., 2022). Results are dependent on spatial scale, with stronger relationships between spectral and field-based diversity observed when the spatial resolution of imagery (i.e., pixel size) matches the size of individual plants (Rossi et al., 2021; Schweiger & Laliberté, 2022; Wang, Gamon, Cavender-Bares, et al., 2018). One recent study across North American biomes found that when the spatial resolution of hyperspectral data was at the m-scale, there was strongest support for SVH in closed-canopy forested ecosystems (Schweiger & Laliberté, 2022). Additionally, relationships can be influenced by factors such as canopy gaps and soils (Gholizadeh et al., 2019; Wang, Gamon, Schweiger, et al., 2018), standing dead biomass (Rossi et al., 2021), and illumination conditions (Hakkenberg, Zhu, et al., 2018)—features that can increase spectral heterogeneity independently of plant traits. This may explain why spectral diversity metrics that more heavily weight extreme spectral values show weaker relationships with field-based diversity (Rossi et al., 2021). Currently, there is no consensus on the most appropriate spectral diversity metric (Wang & Gamon, 2019). Despite criticisms regarding the SVH (e.g., Fassnacht et al., 2022; Schmidlein & Fassnacht, 2017), spectral community properties may prove to be an effective approach to quantifying plant communities in certain ecosystems and under certain conditions.

While imaging spectroscopy is commonly presented as an approach for quantifying temporal changes in communities (e.g., Wang & Gamon, 2019), maps of spectral community properties across broad spatial extents also present a potentially powerful resource for examining ecological processes across space (Cavender-Bares et al., 2017; Kothari & Schweiger, 2022). Field-based studies typically have relatively small sample sizes, which can result in the failure to detect real effects or in the detection of spurious effects (Anderson et al., 2001). Hyperspectral data can greatly increase sample sizes, in addition to incorporating more variation in plant form and function than is typically quantified in field-based studies (Kothari & Schweiger, 2022). Despite calls for a

wider application of hyperspectral data (Cavender-Bares et al., 2017; Kothari & Schweiger, 2022), few studies have explicitly investigated the ability to examine ecological processes (e.g., environmental effects on communities) using spectral community properties, beyond biodiversity–ecosystem functioning relationships (Schweiger et al., 2018; Wallis et al., 2023; Williams et al., 2021). Spectral community properties might advance our understanding of community assembly, but only if spatial patterns in field-based composition and diversity are reproduced when communities are characterized by hyperspectral data.

Here, we use hyperspectral data from an airborne survey in combination with precisely geolocated field data on canopy trees to examine the SVH along a temperate-to-boreal elevation gradient in southern Québec. First, we assessed the degree of association between spectral and field-based properties, defined by both taxonomic and functional dimensions, of canopy tree communities. We tested the strength of relationships using a variety of methods and metrics characterizing composition and diversity. Then we examined whether spatial patterns in spectral community properties could be used to quantify environmental drivers of canopy tree community properties. If there is strong support for the SVH, we expect relationships between field-based community properties and the environment to be reproduced when using spectral community properties. Finally, we compared the predictive ability of hyperspectral data acquired by two imaging spectrometers with differing spectral properties, notably the wavelength region sampled.

METHODS

Study sites

This study was conducted at two protected areas in the northern temperate zone of Québec, Canada: Parc national du Mont-Mégantic (hereafter, Mont Mégantic) and Parc national du Mont-Saint-Bruno (hereafter, Mont St-Bruno; Figure 1). Elevation across Mont Mégantic ranges from 430 to 1105 m above sea level (m asl), corresponding to a mean annual temperature of $\sim 4^{\circ}\text{C}$ at low elevations and $\sim 1^{\circ}\text{C}$ at high elevations (2013–2021, Station IDs IQUBECNO2 and ILAPATRI2, Weather Underground). Along the elevation gradient, the deciduous temperate forest transitions to coniferous, boreal forest. At low elevations, the canopy is primarily composed of *Acer saccharum* Marshall (sugar maple), *Betula alleghaniensis* Britt. (yellow birch), and *Fagus grandifolia* Ehrh. (American beech). While less common, mixed

forest stands also occur at low elevations, commonly along streams, where the predominant conifers are *Abies balsamea* (L.) Mill. (balsam fir) and *Picea rubens* Sarg. (red spruce). At mid-elevations, the canopy is predominantly yellow birch, red spruce, balsam fir, and *Betula papyrifera* Marshall (paper birch). At high elevations, the canopy is predominantly balsam fir, paper birch, and *Sorbus* spp. Mont St-Bruno is less topographically diverse, with elevation ranging from 30 to 208 m asl, and warmer than Mont Mégantic, with a mean annual temperature of $\sim 7^{\circ}\text{C}$ (2010–2020, Weather Station ID 48374, Environment Canada). Canopy composition is like low elevations at Mont Mégantic, where sugar maple is abundant and grows alongside American beech and more-southerly species, such as *Quercus rubra* L. (red oak), *Ostrya virginiana* (Mill.) K. Koch (American hop-hornbeam), and *Tilia americana* L. (American basswood) occurring at the northernmost limit of their ranges.

Data

During the summers of 2019 and 2020, we established forest inventory plots to span a wide range of conditions present across Mont Mégantic ($n = 50$) and Mont St-Bruno ($n = 15$). Specifically, forest inventory plots were established to (1) maximize the range of unique tree species assemblages sampled and (2) cover the range of environmental conditions (e.g., elevation, slope, and aspect). Plots were $\sim 706\text{ m}^2$ circles (15 m radii) as viewed from above, and dimensions were corrected to account for slope in the field. To relate field data with remotely sensed data, we estimated high-accuracy positions of plot centers (mean horizontal accuracy = 0.2 m; Trimble Catalyst DA1 antenna with Trimble RTX correction service, Trimble Inc.).

Taxonomic dimension

Within each forest inventory plot, we quantified the tree community—all individuals with crowns extending into the upper canopy, as well as individuals with lower crowns having a dbh ≥ 9 cm. All individuals were identified to species and positioned in relation to plot center, dbh and height were quantified and assigned a canopy class (i.e., a categorical variable that describes the vertical position and dominance of crowns; classes defined by NRCan, 2008), and a suite of crown measurements required to model crown area and position crowns in relation to their trunks were quantified (detailed in Crofts et al., 2022).

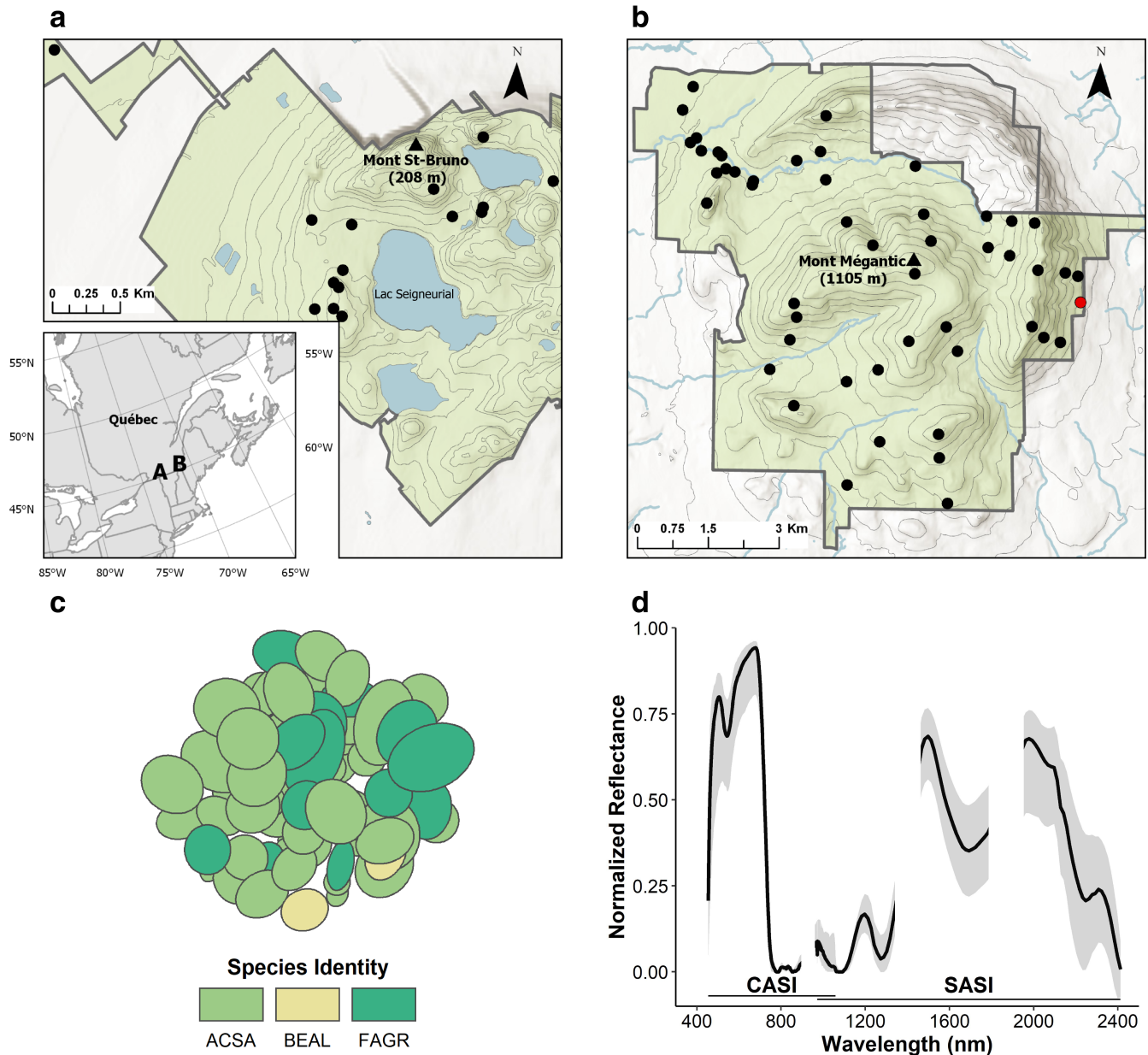


FIGURE 1 Maps of forest inventory plots surveyed at the two study sites: (a) Parc national du Mont-Saint-Bruno ($n = 15$) and (b) Parc national du Mont-Mégantic ($n = 50$); locations within southern Québec, Canada, are depicted in the inset map. The parks' extent is represented by the green shading, and forest inventory plots are symbolized by the black dots. The red dot symbolizes the plot for which (c) taxonomic composition and (d) spectral composition are exemplified. (c) The plot's taxonomic composition, where bird's-eye-view ellipses are modeled tree crowns and color represents species identity (ACSA = *Acer saccharum*, BEAL = *Betula alleghaniensis*, FAGR = *Fagus grandifolia*). (d) The plot's normalized reflectance spectrum (see *Methods* for details), where the gray interval represents the range of values observed across all spectral points within the plot and the black line represents the mean normalized reflectance. The visible to near-infrared regions were sampled by the Compact Airborne Spectrographic Imager (CASI-1500; 454–1059 nm), and the shortwave infrared region was sampled by the Shortwave Infrared Airborne Spectrographic Imager (SASI-640; 972.5–2412.5 nm). Gaps in the normalized reflectance spectrum correspond to bands that were masked due to low signal-to-noise ratio or water absorption features.

Given that only the uppermost layer of vegetation is captured by imaging spectrometers, for the analyses we considered the subset of trees forming the uppermost layer of the canopy. To do so, we modeled tree crowns as ellipses, positioned crowns in relation to their associated

tree trunks, and determined their vertical order based on canopy class and height (Figure 1c). When crowns overlapped, we retained the entire area of the overlapping region for the uppermost individual, but we clipped the overlapping region from the crowns of all

underlying individuals so only the area of their crowns as we would expect to be visible from above remained (detailed in Wallis et al., 2023). We calculated relative species abundance per plot as the sum of a species' as-visible-from-above crown area divided by the total as-visible-from-above crown area.

Functional dimension

For all species observed within the forest inventory plots, we calculated species' mean trait values for 15 foliar traits using the Canadian Airborne Biodiversity Observatory's (CABO; www.caboscience.org) foliar trait database. Species mean trait values were calculated using all individual trees of each species within the CABO database sampled during the 2018 and 2019 growing seasons (30 June–1 September); this included individuals sampled from the study sites and surrounding regions in southern Québec (Appendix S1: Tables S3–S5). Leaf sampling and trait quantification followed CABO's standardized protocols (detailed in Kothari et al., 2023). Mature, healthy, and fully sunlit leaves were harvested and bulked at the level of individuals. For each bulk leaf sample, we quantified foliar traits characterizing dry matter and water (i.e., specific leaf area [SLA], leaf dry matter content [LDMC], relative water content [RWC], and equivalent water thickness [EWT]); carbon (C) and nitrogen (N) concentrations; carbon fraction concentrations (i.e., soluble contents, hemicellulose, cellulose, lignin, and recalcitrant); and pigment concentrations (i.e., chlorophyll *a* [chl *a*], chlorophyll *b* [chl *b*], chl *a* to chl *b* ratio, and carotenoid concentration). Biochemical concentrations are expressed per unit mass. We calculated the community weighted mean (CWM) values for each foliar trait per forest inventory plot, where species mean trait values were weighted by species' relative abundances as visible from above per plot.

Spectral dimension

Hyperspectral data were acquired as part of the CABO project during the growing season when deciduous leaves were fully opened and matured (Mont Mégantic: 18 July 2019, Mont St-Bruno: 8 September 2018) by the National Research Council of Canada's Flight Research Lab (Appendix S1: Section S1). Two imaging spectrometers mounted on a Twin Otter fixed-wing aircraft were used to acquire hyperspectral data: the Compact Airborne Spectrographic Imager (CASI-1500) and the Shortwave Infrared Airborne Spectrographic Imager (SASI-640; ITRES, Calgary, AB, Canada). The CASI-1500 samples

288 spectral channels covering the visible to near-infrared (VNIR) wavelengths (375.28–1061.46 nm), and the SASI-640 samples 100 spectral channels covering the SWIR wavelengths (957.5–2442.5 nm). The raw hyperspectral data underwent standard processing steps (detailed in Inamdar et al., 2021). It was radiometrically corrected using proprietary software developed by the sensor manufacturer, atmospherically corrected using ATCOR4 (Soffer et al., 2019), and geometrically corrected using a digital surface model (DSM), created from light detection and ranging (LiDAR) data, produced by the Québec provincial government (see Inamdar et al. [2021] for correction methodology; DSM available at: <https://www.foretouverte.gouv.qc.ca/>; Leboeuf et al., 2015). Additionally, we applied a Lambert + Statistical-Empirical bidirectional reflectance distribution function topographic correction (Richter & Schläpfer, 2020). We used directly georeferenced hyperspectral point clouds (DHPCs) rather than the more common raster format because DHPCs preserve the spatial-spectral integrity of the hyperspectral data without shifts, loss, or duplication of spectral measurements, which can be particularly problematic across topographically complex terrain when resampling to uniform, square pixels (Inamdar et al., 2021). The raw pixel sizes of the two sensors differ and thus are not spatially aligned (Appendix S1: Table S1). While hyperspectral reflectance across the full spectrum (400–2400 nm) might be advantageous (but see Imran et al., 2021), we chose not to spatially resample and fuse the data sets because conventional spatial resampling approaches fail to account for the spatial characteristics of the coarser-resolution imager (i.e., spatial point spread function; Inamdar et al., 2023). Moreover, preliminary examinations of our data suggested that the magnitude of support for the SVH tended to be weaker when spectral community properties were quantified using the full-range hyperspectral data (Appendix S1: Section S2). To this extent, the two separate DHPC products composed of either CASI-1500 or SASI-640 data were analyzed separately.

We extracted all spectral points from DHPCs that covered the forest inventory plots and applied common postprocessing steps. In brief, we masked shadowed and nonforested spectral points, excluded low-signal and noisy regions of the spectra, including the water absorption regions, and applied a smoothing filter (detailed in Appendix S1: Section S1). Additionally, to minimize differences due to potentially varying illumination conditions during acquisition, we normalized the spectra via continuum removal using the convex hull band depth method in the *hsdar* R package (Lehnert et al., 2019). The resulting spectral data sets contained the normalized reflectance at 229 bands spanning 454–1059 nm for the CASI-1500 data set and 78 bands

spanning 972–2412 nm for SASI-640 data set for all nonshadowed, forested points covering the forest inventory plots (Figure 1d). Going forward, we will refer to the spectral data sets by the wavelength regions in which they encompass VNIR (CASI-1500 data set) and SWIR (SASI-640 data set).

Abiotic environment

To quantify the abiotic conditions within each forest inventory plot, we calculated a suite of environmental variables using the terra R package (Hijmans, 2023) from LiDAR data products created by the Québec provincial government (Tile IDs 21E06NE and 31H11SO for Mont Mégantic and Mont St-Bruno, respectively, available at: <https://www.foretouverte.gouv.qc.ca/>; Leboeuf et al., 2015). We derived elevation, slope, roughness, northness, and eastness from a digital terrain model, and averaged values across all pixels per plot. Roughness was calculated as the difference between the maximum and minimum values of a cell and its eight surrounding cells (Wilson et al., 2007). Northness and eastness describe aspect in a linear way, where northness was calculated as the cosine of aspect and eastness as the sine of aspect. Additionally, we calculated the average topographic wetness index (TWI) per plot from a TWI model.

Statistical analyses

Degree of correspondence

To examine the degree of correspondence between spectral and field-based composition, we first took a multivariate approach in which we conducted four symmetric Procrustes analyses, comparing the two assessments of spectral composition (VNIR and SWIR) with two field-based assessments of composition (taxonomic and functional) across all plots ($n = 65$) using the vegan R package (Oksanen et al., 2022). Procrustes analyses quantify the similarity in structure between two data sets that describe the same objects (in this case plots); the data sets of interest are first subject to ordination analyses and then the ordinations undergo a “Procrustes” transformation, in which they are scaled, rotated, and dilated to minimize the residual sum-of-squared distances between the pairs of points (one pair for each plot) (Legendre & Legendre, 2012). We used principal component analyses (PCA) to ordinate the data sets using the vegan R package (Oksanen et al., 2022). Prior to conducting PCAs, we Hellinger-transformed species abundances, centered and

standardized trait CWMs, and calculated the mean normalized reflectance at each band per forest inventory plot for the spectral data sets. We used the eight principal component (PC) axes explaining more than 90% of the variation and examined the significance of association between the two data sets via permutation ($n = 999$). We then examined the degree of linear association between the PC axes across data sets using Pearson’s correlations in the stats R package (R Core Team, 2021).

We examined multiple commonly used metrics per dimension, based on different elements of diversity (e.g., richness, evenness, and divergence) (Table 1). To examine the strength and direction of linear associations between spectral and field-based diversity, we estimated Pearson’s correlations between all spectral diversity metrics and taxonomic or functional diversity metrics ($n = 59$ – 65 plots; dependent on diversity metric, given mathematical constraints relating to the minimum number of species). Taxonomic diversity metrics were calculated using the hillR R package (Li, 2018), except for Pielou’s evenness, which was calculated using basic operations in R (R Core Team, 2021). Functional diversity metrics were calculated using the FD R package (Laliberté et al., 2014). Spectral diversity metrics were calculated using custom functions in R (R Core Team, 2021). The functions for the coefficient of variation (CV) and convex hull volume (CHV) included a rarefaction step to standardize the number of spectral points per forest inventory plot, where we randomly selected spectral points equal to the minimum number of spectral points observed across all plots ($n = 110$ for VNIR; $n = 95$ for SWIR) and then calculated the spectral diversity metrics. The rarefaction was repeated 999 times, and we averaged the spectral diversity metrics across all iterations. For CHV, the rarefaction step occurred after computing the PCs. Spectral variance (SV) is standardized by the number of spectral points, so we did not include the rarefaction step. One forest inventory plot only contained one species, and therefore, the exponential Shannon index (1D), inverse Simpson’s index (2D), Pielou’s evenness (J'), functional dispersion (F_{Dis}), and Rao’s entropy (RaoQ) could not be quantified ($n = 64$). Moreover, functional richness (F_{Ric}), functional evenness (F_{Eve}), and functional divergence (F_{Div}) could not be quantified for six plots that contained fewer than three species ($n = 59$). To identify the wavelengths contributing most to spectral diversity, we calculated the variance in normalized reflectance at each band for each forest inventory plot.

We use the following terms to describe the observed strength of association: weak ($r \leq 0.3$), moderate ($r = 0.31$ – 0.6), and strong ($r \geq 0.61$).

TABLE 1 Description of diversity metrics examined in this study.

Diversity metric	Symbol	Formula/definition	Reference
Taxonomic			
Species richness	0D	${}^0D = S = \sum_{i=1}^S p_i^0$	Hill (1973), MacArthur (1965)
Exponential Shannon's index	1D	${}^1D = \exp\left(-\sum_{i=1}^S p_i \log p_i\right)$	Hill (1973), MacArthur (1965)
Inverse Simpson's index	2D	${}^2D = 1/\sum_{i=1}^S p_i^2$	Hill (1973), MacArthur (1965)
Pielou's evenness index	J'	$J' = \ln {}^1D / \ln S$	Pielou (1966)
Functional			
Functional richness	F_{Ric}	Amount of functional space filled by a community, calculated as convex hull volume of species in functional space	Villéger et al. (2008)
Functional evenness	F_{Eve}	Regularity of distribution of trait abundances in functional space, calculated as minimum sum of branch lengths of minimum spanning tree that links all species, weighted by relative abundance of species	Villéger et al. (2008)
Functional divergence	F_{Div}	Spread of distribution of trait abundances in functional space, calculated as deviation of species from minimal distance to center of gravity, weighted by their relative abundance	Villéger et al. (2008)
Functional dispersion	F_{Dis}	Spread of distribution of trait abundances in functional space, calculated as mean distance of species from centroid of all species, weighted by their relative abundance	Laliberté and Legendre (2010)
Rao's entropy	RaoQ	Spread of distribution of trait abundances in functional space, calculated as sum of distances between species pairs weighted by their relative abundance	Botta-Dukát (2005)
Spectral			
Convex hull volume	CHV	Amount of spectral space filled by a community, calculated as CHV of first three principal components of spectral reflectance data	Dahlin (2016)
Coefficient of variation	CV	$CV = \frac{\sum_{j=1}^b s(y_j) / \bar{y}_j}{b}$	Wang et al. (2016)
Spectral variance	SV	$SV = \frac{\sum_{j=1}^b \sum_{i=1}^m (y_{ij} - \bar{y}_j)^2}{m-1}$	Laliberté et al. (2020)

Note: S = number of species observed; p_i = relative abundance of i th species; y_j = reflectance of j th band; b = number of spectral bands; y_{ij} = reflectance of i th pixel/spectral point at j th band; m = number of pixels/spectral points.

Environmental drivers of community properties

To examine whether the relationships between field-based community properties and the environment can be effectively captured using hyperspectral data, we compared how the composition and diversity of each biodiversity dimension varied along environmental gradients at Mont Mégantic. We used redundancy analyses (RDAs) to examine the relationships between

composition and environment and general additive models (GAMs) to examine the relationships between diversity and environment. Environmental variables were examined for collinearity, and the variables retained as explanatory factors were elevation, slope, northness, eastness, and TWI ($|r| < 0.7$). Explanatory factors were centered and standardized prior to analyses.

We conducted separate RDAs to evaluate how environmental conditions influenced taxonomic, functional,

and spectral composition using the *vegan* R package (Oksanen et al., 2022). We used permutation to test the significance of the fit of the overall models, individual canonical axes, and explanatory variables ($n = 999$). Like the Procrustes analyses, we Hellinger-transformed species abundances, centered and standardized trait CWMs, and calculated the mean normalized reflectance at each band per forest inventory plot for the spectral data sets prior to conducting RDAs.

We ran separate GAMs to evaluate how environmental conditions influenced taxonomic, functional, and spectral diversity using the *mgcv* R package (Wood, 2011). We focused on one diversity metric per biodiversity dimension, based on the strength of spectral-field-based diversity relationships and the degree of use in the literature: exponential Shannon index (1D), functional dispersion (F_{Dis}), and spectral variance (SV). GAM is a nonparametric regression method where the relationship between explanatory variables and the response variable is modeled using smooth functions, which can be linear or nonlinear (Larsen, 2015). We chose to model diversity using GAMs due to the markedly nonlinear diversity–elevation relationship; all other abiotic predictors were modeled as linear. We used penalized regression splines as the smoothing function and estimated smoothing parameters for elevation using restricted maximum likelihood (REML). To identify the relative importance of environmental variables in a manner comparable across models, we calculated the proportion of deviance explained by each explanatory variable. Model assumptions were checked visually from diagnostic residual plots, and smoothing parameters were checked using the *k*-index ratio. All statistical analysis were conducted in R version 4.1.0 (18 May 2021) (R Core Team, 2021).

RESULTS

Degree of correspondence

Composition

In multivariate analyses, spectral composition was moderately associated with field-based composition (Procrustean $r = 0.50$ – 0.59), as based on the first eight PC axes that cumulatively explained >90% of the variation of each dimension (herein referred to as “total” composition). The degree of association was marginally stronger when “total” spectral composition was characterized using VNIR wavelengths (average Procrustean $r = 0.56$) than when using SWIR wavelengths (average Procrustean $r = 0.52$). Across the VNIR wavelengths, “total” spectral composition was marginally more associated with “total” taxonomic

composition than with “total” functional composition (Procrustean $r = 0.59$, $p = 0.001$ and Procrustean $r = 0.53$, $p = 0.001$, respectively). Across the SWIR wavelengths, “total” spectral composition was similarly associated with “total” taxonomic composition and “total” functional composition (Procrustean $r = 0.52$, $p = 0.001$ and Procrustean $r = 0.50$, $p = 0.001$, respectively).

Generally, the degree of association between spectral and field-based composition increased when only considering the major axes of compositional variation. The main axis of taxonomic composition explained 48.6% of the overall variation, characterizing a gradient from deciduous, temperate forest communities to mostly coniferous, boreal forest communities (Figure 2a). Similarly, the main axis of functional composition explained 58% of the overall variation, based on intercorrelated traits known to differ between broadleaves and needle leaves (Figure 2b). The main axis of spectral composition across the VNIR wavelengths explained 84.6% of the variation and showed high negative scores across the visible wavelengths (Figure 2c), while the main axis of spectral composition across the SWIR wavelengths explained 59% of variation and was characterized by positive scores at longer wavelengths with a peak at 2200 nm.

Across the VNIR wavelengths, the main axis of spectral composition was strongly associated with the main axis of taxonomic composition ($r = 0.65$, $p < 0.001$) and more strongly associated with the main axis of functional composition ($r = 0.79$, $p < 0.001$). Across the SWIR wavelengths, the main axis of spectral composition was not associated with the main axis of taxonomic composition ($r = -0.05$, $p = 0.702$) or the main axis of functional composition ($r = 0.02$, $p = 0.849$). However, the secondary axis for SWIR-spectral composition was strongly associated with the main axis of taxonomic composition ($r = -0.75$, $p < 0.001$) and the main axis of functional composition ($r = -0.77$, $p < 0.001$). The secondary axis of SWIR-spectral composition explained 28% of variation and was characterized by peaks at multiple wavelengths (Figure 2d). See Appendix S1: Figure S5 for correlation matrix of the first three PCs across spectral and field-based dimensions.

Diversity

Spectral diversity metrics were predominantly positively related to taxonomic and functional diversity metrics; however, the strength of association varied across spectral metrics and the field-based metrics to which they were compared (Figure 3; Table 2). On average, the degree of association between spectral diversity and field-based diversity was similar for taxonomic diversity (average $r = 0.319$) and functional diversity (average

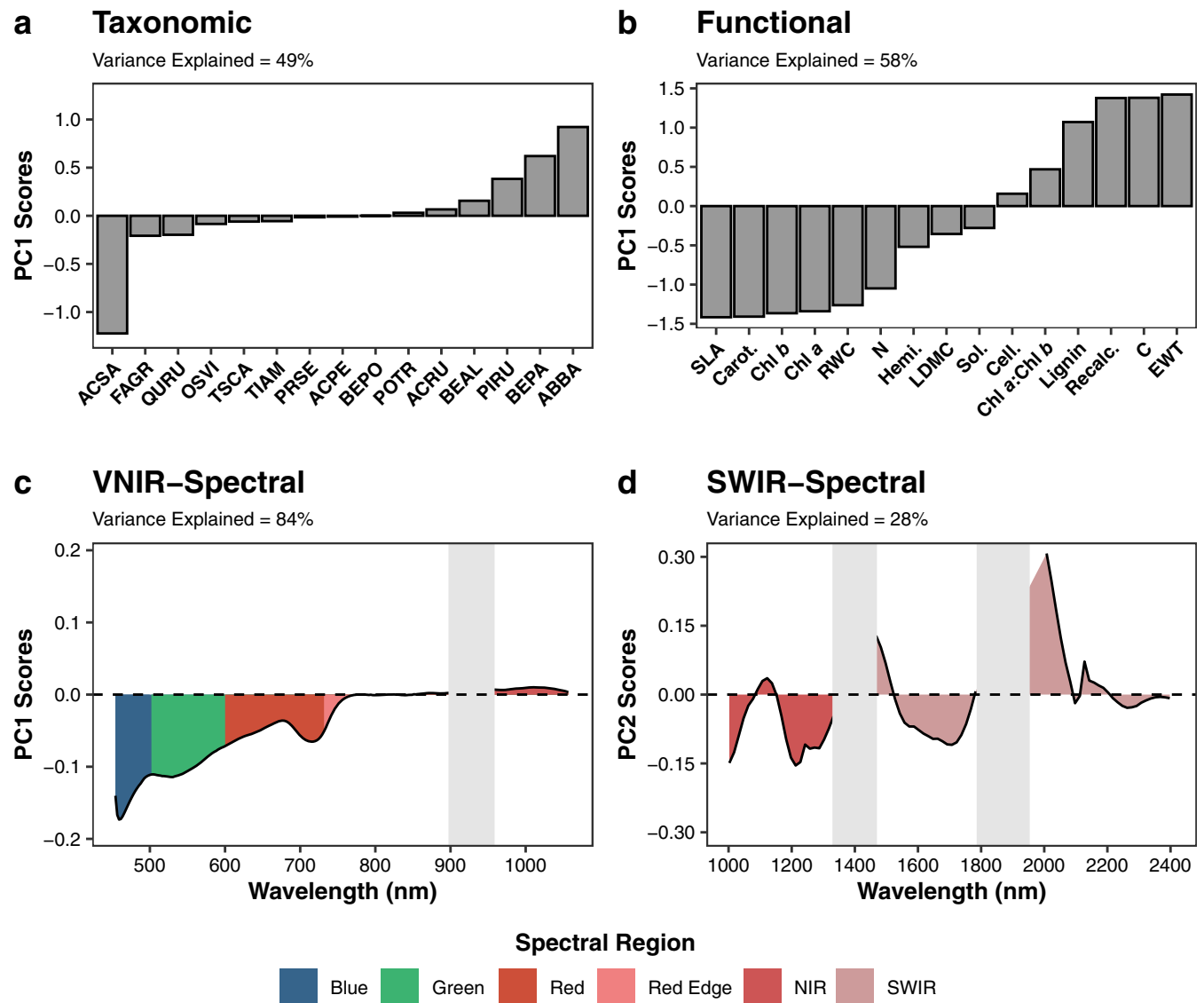


FIGURE 2 Ordination scores along correlated principal component (PC) axes of (a) 15 most abundant tree species along first taxonomic PC axis, (b) leaf functional traits along first functional PC axis, (c) normalized reflectance across visible to near-infrared (VNIR) spectral wavelength bands along the first VNIR-spectral PC axis, and (d) normalized reflectance across shortwave infrared (SWIR) spectral wavelength bands along second SWIR-spectral PC axis. Species acronyms: ACSA = *Acer saccharum*, FAGR = *Fagus grandifolium*, QURU = *Quercus rubra*, OSVI = *Ostrya virginiana*, TSCA = *Tsuga canadensis*, TIAM = *Tilia americana*, PRSE = *Prunus serotina*, ACPE = *A. pensylvanicum*, BEPO = *Betula populifolia*, POTR = *Populus tremuloides*, ACRU = *A. rubrum*, BEAL = *B. alleghaniensis*, PIRU = *Picea rubens*, BEPA = *B. papyrifera*, and ABBA = *Abies balsamea*. Functional trait acronyms: SLA = specific leaf area, Carot. = carotenoid content, Chl *b* = chlorophyll *b* content, Chl *a* = chlorophyll *a* content, RWC = relative water content, N = nitrogen content, Hemi. = hemicellulose content, LDMC = leaf dry mass content, Sol. = soluble carbon content, Cell. = cellulose content, Chl *a*:Chl *b* = ratio of chlorophyll *a* to *b*, Lignin = lignin content, Recalc. = recalcitrant content, C = carbon content, and EWT = equivalent water thickness.

$r = 0.327$; Figure 3). Field-based diversity metrics were on average more strongly associated with spectral diversity metrics summarizing VNIR wavelengths (average $r = 0.382$) than those summarizing SWIR wavelengths (average $r = 0.265$; Figure 3). However, the relative performance of different spectral diversity metrics was similar regardless of the hyperspectral data they summarized or the field-based metric to which they were compared;

on average the CV was more weakly associated with field-based diversity metrics than either CHV or SV (average $r = 0.209$, average $r = 0.379$, and average $r = 0.382$, respectively; Figure 3). Henceforth, for spectral diversity we will focus on the CHV and SV as quantified by normalized reflectance across the VNIR wavelengths.

Spectral diversity was moderately associated with taxonomic diversity metrics ($r = 0.336$ – 0.559 ; Table 2,

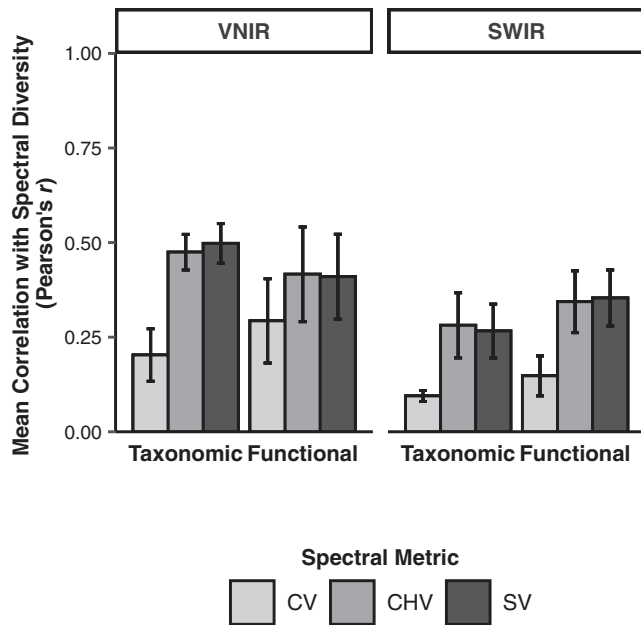


FIGURE 3 Mean Pearson's correlation with spectral diversity derived from visible to near-infrared and shortwave infrared wavelengths as calculated as coefficient of variation (CV), convex hull volume (CHV), and spectral variance (SV) across field-based diversity derived from taxonomic ($n = 4$) and functional ($n = 5$) diversity metrics. Error bars represent SE.

Appendix S1: Figure S6). Species richness (0D) showed the lowest correlations of the taxonomic metrics, where Pielou's evenness (J'), exponential Shannon's index (1D), and inverse Simpson's index (2D) were approximately 1.6 times more strongly correlated to spectral diversity than species richness (Table 2). Similarly, spectral diversity was moderately to strongly associated with functional diversity metrics ($r = 0.348$ – 0.676), except for functional divergence (F_{Div}), which was not significantly related to spectral diversity (Table 2, Appendix S1: Figure S6). Of all the field-based diversity metrics examined, Rao's entropy (RaoQ) and functional dispersion (F_{Dis}), which incorporate functional richness and divergence, showed the strongest correlations with spectral diversity (Table 2). Functional richness (F_{Ric}) was approximately 1.5 times less associated with spectral diversity than RaoQ and functional dispersion (F_{Dis}) but was more associated with spectral diversity than functional evenness (F_{Eve}) (Table 2).

Environmental drivers of community properties

Composition

The environmental predictors explained 27% of the variation in taxonomic composition (pseudo- $F = 4.65$,

$p < 0.001$), 28% of the variation in functional composition (pseudo- $F = 4.90$, $p < 0.001$), and 44% of the variation in VNIR-spectral composition (pseudo- $F = 8.60$, $p < 0.001$; Figure 4). The first canonical axis explained 21% of total variation in taxonomic composition, 22% of functional composition, and 41% of VNIR-spectral composition (Figure 4). The second canonical axis explained relatively little variation in composition, accounting for 5% of total taxonomic variation and 6% of total functional variation (Figure 4). For VNIR-spectral composition, the second canonical axis explained 3% of total compositional variation, too little to interpret ($< 5\%$, as defined by Legendre et al. [2011]). While spectral composition across the SWIR wavelengths was significantly affected by environmental conditions, only 11% of the variation in SWIR-spectral composition was explained by the environmental predictors (pseudo- $F = 2.30$, $p = 0.02$). Given that the vast majority of SWIR-spectral composition is not explained by environmental predictors (~20% more unconstrained variance than the other dimensions; Appendix S1: Table S3) and the relatively weak statistical support for the canonical relationship, we do not interpret the canonical axes for this aspect of spectral composition.

The relationships between environmental predictors and field-based composition tended to be reproduced by VNIR-spectral composition, in terms of the relative explanatory power and the effect on percent coniferous cover. Elevation explained the majority of fitted variance in taxonomic, functional, and VNIR-spectral composition; however, elevation explained ~20% more fitted variance in VNIR-spectral composition than either taxonomic or functional composition (Table 3). Across the dimensions, elevation was strongly correlated with the first canonical axis that separated broadleaved, deciduous temperate plots from evergreen, coniferous boreal plots (average $|r| = 0.821$; Figure 4). For the taxonomic and functional dimensions, elevation was moderately associated with the second canonical axis that separated mixed forest plots from unmixed forest plots (i.e., either broadleaved or coniferous) (average $|r| = 0.620$; Figure 4). Northness explained the second most fitted variance in taxonomic and functional composition, but it did not affect VNIR-spectral composition (Table 3). For the taxonomic and functional dimensions, northness was strongly correlated with the second canonical axis (average $|r| = 0.712$; Figure 4). Across the dimensions, slope explained ~13% of fitted variance in taxonomic, functional, and VNIR-spectral composition (Table 3) and was strongly correlated with the second canonical axis (average $|r| = 0.664$; Figure 4).

TABLE 2 Degree of linear association between field-based diversity metrics and spectral diversity metrics, which summarize (a) the visible to near-infrared (VNIR) wavelengths or (b) the shortwave infrared (SWIR) wavelengths, as determined by Pearson's correlation ($n = 59\text{--}65$, dependent on field-based diversity metric).

Spectral region	Field-based dimension	Field-based metric	Correlation with spectral diversity (Pearson's r)		
			CV	CHV	SV
VNIR	Taxonomic	0D	0.036	0.336	0.341
		1D	0.192	0.521	0.539
		2D	0.199	0.520	0.551
		J'	0.381	0.531	0.559
	Functional	F_{Ric}	0.339	0.428	0.452
		F_{Eve}	0.349	0.348	0.358
		F_{Div}	−0.14	−0.017	0.007
		F_{Dis}	0.443	0.646	0.611
	RaoQ	0.475	0.676	0.621	
SWIR	Taxonomic	0D	0.155	0.065	0.077
		1D	0.189	0.276	0.270
		2D	0.174	0.301	0.296
		J'	0.233	0.485	0.422
	Functional	F_{Ric}	0.156	0.299	0.264
		F_{Eve}	−0.035	0.403	0.419
		F_{Div}	0.118	0.047	0.105
		F_{Dis}	0.240	0.493	0.492
	RaoQ	0.260	0.477	0.486	

Note: Bold values represent statistically significant values ($p < 0.05$) as determined by two-sided t -test. Taxonomic diversity metrics examined were species richness (0D), exponential Shannon's index (1D), inverse Simpson's index (2D), and Pielou's evenness (J'), and functional diversity metrics were functional richness (F_{Ric}), functional evenness (F_{Eve}), functional divergence (F_{Div}), functional dispersion (F_{Dis}), and Rao's entropy (RaoQ). Spectral diversity metrics examined were coefficient of variation (CV), convex hull volume (CHV), and spectral variance (SV).

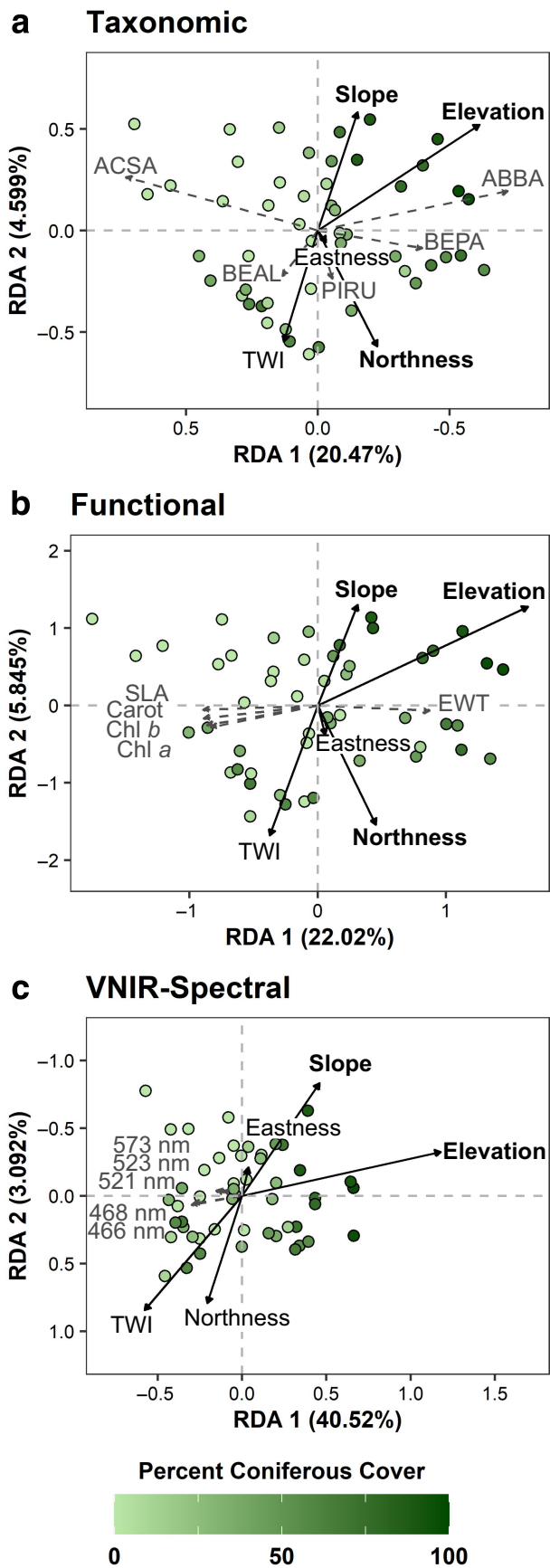
Diversity

The relationships between field-based diversity and environmental predictors were generally reproduced when using spectral diversity composed of the VNIR wavelengths, both in terms of their relative explanatory power and the shape of the relationships (Table 4; Figure 5; Appendix S1: Figure S7). However, the absolute explanatory power of environmental predictors differed between field-based and spectral diversity. Environmental predictors explained the majority of observed variation in field-based diversity, explaining 65% of the variation in taxonomic diversity and 49% of the variation in functional diversity but only 32% of the variation in VNIR–spectral diversity and 35% of SWIR–spectral diversity. Elevation explained the majority of the fitted variation in taxonomic, functional, and VNIR–spectral diversity (Table 4). Across these dimensions, the elevation–diversity relationship was multimodal, with peaks at low elevation along the valley bottom (average

elevation = 472 m; average slope = 6°) and at mid-elevations (average elevation = 826 m; average slope = 15° ; Figure 5). Northness explained the second most fitted variation in taxonomic, functional, and VNIR–spectral diversity; however, the effect on taxonomic diversity was weak and lacked statistical support (Table 4). Functional and VNIR–spectral diversity increased with northness (Appendix S1: Figure S7). In contrast, northness and elevation explained similar proportions of fitted variance in SWIR–spectral diversity (Table 4).

DISCUSSION

We analyzed the link between spectral and field-based expressions of canopy tree biodiversity and examined the ability to use spectral properties to predict environmental drivers of canopy tree communities along a temperate-to-boreal gradient. Overall, we found support for the SVH and aligned with theory: Spectral community



properties tended to be more tightly associated with functional than taxonomic community properties. However, the degree of association was highly variable and was dependent on the method or metric used to quantify composition or diversity, respectively. To the best of our knowledge, we are the first to examine the relationship between spectral diversity and field-based metrics that quantify different elements of functional diversity; spectral diversity was most strongly associated with metrics that quantify functional richness and divergence. We also found that the relationships between field-based community properties and the environment were effectively reproduced when using hyperspectral data. Spatial trends in canopy tree composition and diversity were strongly associated with the turnover from temperate to boreal communities along the elevation gradient. Overall, our results suggest that imaging spectroscopy is a useful tool to study biodiversity-environment relationship in northern temperate forests, even in the absence of forest inventory field data.

Degree of correspondence

Effect of field-based dimension on spectral-field based relationship

In agreement with theory, we found that the degree of association between spectral and field-based community properties was generally greater for the functional than the taxonomic dimension (Kothari & Schweiger, 2022; Ustin & Gamon, 2010). Despite the understanding that traits causally drive plant-light interactions, most tests of the SVH have been limited to relating the spectral dimension with the taxonomic dimension (Fassnacht et al., 2022). While species differ in their trait values, the discrete nature of species identities assumes that all species are equally (dis)similar in phenotype, whereas trait

FIGURE 4 Redundancy analysis (RDA) triplots with type 2 scaling depicting the relationships between environmental predictors and (a) taxonomic, (b) functional, and (c) visible to near-infrared (VNIR)-spectral composition ($n = 50$). Solid black arrows: effect of environmental predictors; gray dashed arrows: response scores of five most correlated (a) species (ABBA = *Abies balsamea*, ACSA = *A. saccharum*, BEAL = *Betula alleghaniensis*, BEPA = *B. papyrifera*, and PIRU = *Picea rubens*), (b) traits (Carot = carotenoid content, Chl a = chlorophyll a content, Chl b = chlorophyll b content, EWT = equivalent water thickness, SLA = specific leaf area), and (c) wavelengths. Length of arrow represents strength of correlation of that variable with canonical axes and points are the fitted plot scores.

TABLE 3 Proportion of fitted variance (%) that each environmental predictor variable accounted for in taxonomic composition, functional composition, and visible to near-infrared (VNIR)–spectral composition as determined by marginal effects of redundancy analyses (RDAs).

Parameter	Proportion of explained variance (%)		
	Taxonomic composition	Functional composition	VNIR–spectral composition
Elevation	59.59	63.71	83.32
Northness	21.98	18.43	2.98
Slope	12.65	13.91	12.22
TWI	3.45	2.07	0.97
Eastness	2.33	1.88	0.56

Note: Bold values represent statistically significant values as determined by Monte Carlo permutation testing ($n = 999$). For detailed model outputs, see Appendix S1: Table S4.

Abbreviation: TWI, topographic wetness index.

TABLE 4 Proportion of explained deviance (%) that each environmental predictor variable accounted for in taxonomic diversity (exponential Shannon's Index; 1D), functional diversity (functional dispersion; F_{Dis}), visible to near-infrared (VNIR)–spectral diversity (spectral variance [SV]), and shortwave infrared (SWIR)–spectral diversity (SV) as determined by general additive models [GAMs]; $n = 50$).

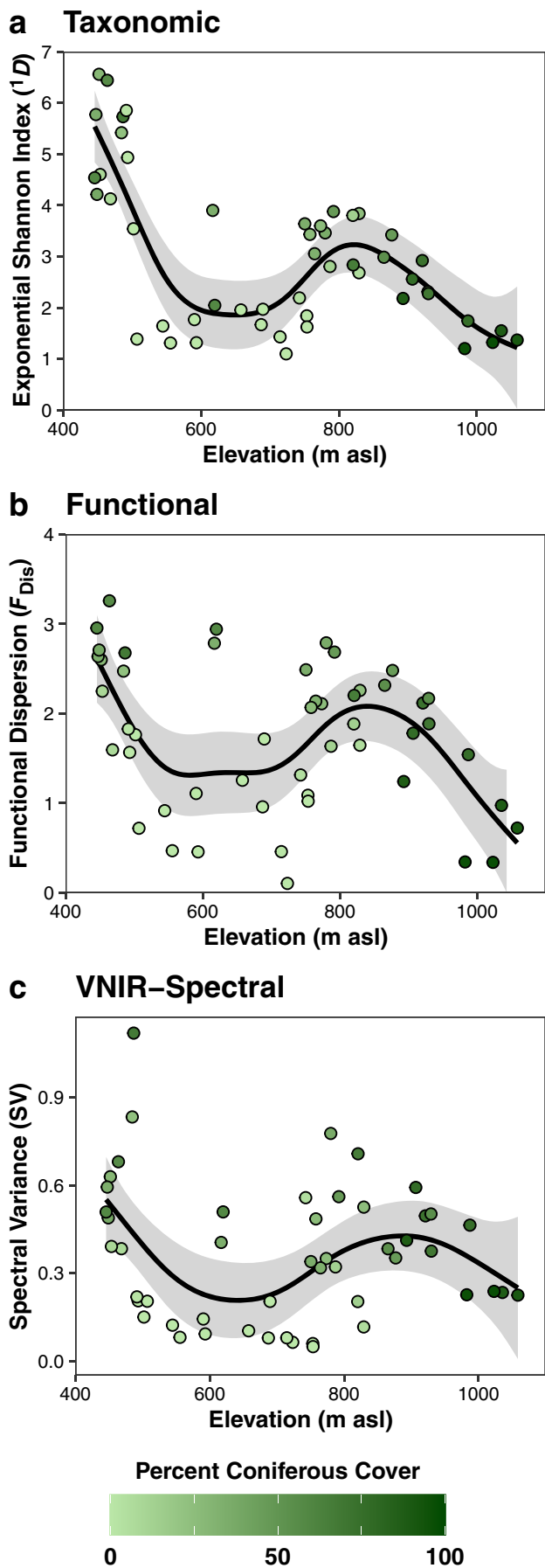
Parameter	Proportion of explained deviance (%)			
	Taxonomic diversity (1D)	Functional diversity (F_{Dis})	VNIR–spectral diversity (SV)	SWIR–spectral diversity (SV)
Elevation	93.68	71.72	67.41	47.36
Northness	4.74	26.11	22.20	47.67
Eastness	1.18	0.63	1.98	0.16
Slope	0.35	1.59	8.61	4.14
TWI	0.05	−0.06	−0.20	0.67

Note: Bold values represent statistically significant values. For detailed model outputs, see Appendix S1: Table S5.

Abbreviation: TWI, topographic wetness index.

values and hyperspectral reflectance continuously describe phenotypic (dis)similarity. Surprisingly, of the studies that also examined the spectral–functional relationship, support for the SVH has not been consistently stronger for the functional dimension (e.g., Kamoske et al., 2022). We demonstrate that choice of method or metric affects the degree of association between spectral and field-based dimensions (described below). When the SVH has been examined beyond the taxonomic dimension, the functional dimension has been characterized by a single diversity metric (e.g., Frye et al., 2021; Kamoske et al., 2022), and differences in functional diversity metric choice may explain inconsistencies in the spectral–functional relationship. Additionally, the functional dimension requires judgment as to which traits to include, making it difficult to compare studies that use different traits (van der Plas et al., 2020; Zhu et al., 2017). Here, the functional dimension is composed of a suite of foliar leaf traits causally associated with foliar reflectance, including

traits that are not commonly quantified, such as carbon fractions and pigment concentrations (Kattge et al., 2020), under the expectation that these traits would be closely related to the spectral dimension. Trait choice likely affects the spectral–functional relationship, and we argue that the inclusion of traits not related to plant–light interactions (e.g., rooting depth, lifespan, seed dry mass) could weaken the association between the spectral and functional dimensions (e.g., Kamoske et al., 2022). In circumstances where trait data are limited, characterizing communities using the phylogenetic dimension may advance the understanding of how spectral community properties relate to field-based community properties, as phylogenetic relatedness can capture evolved differences in traits (e.g., Schweiger & Laliberté, 2022; Wang, Gamon, Schweiger, et al., 2018). However, the phylogenetic–spectral relationship is indirect, and mismatches between genotype and phenotype (e.g., convergent evolution, phenotypic plasticity) may weaken the degree of association (Ollinger, 2011).



Effect of methods on spectral-field-based composition relationship

Spectral composition is a relatively new concept compared to spectral diversity, and, so far, the SVH has rarely been extended to examine its relationship with field-based composition (but see Draper et al., 2019; Féret & Asner, 2014; Hakkenberg, Peet, et al., 2018; Schweiger & Laliberté, 2022; Wallis et al., 2023). We found that the maximum correspondence between spectral and field-based composition was greater when relating ordination scores of primary axes of compositional variation (i.e., bivariate relationships) than when relating “total” composition (i.e., ordination axes that cumulatively accounted for >90% of compositional variation) using a multivariate approach. However, when relating the primary axes of compositional variation, the strength of association was dependent on the wavelength regions that composed spectral composition and the field-based dimension to which it was compared but was not when relating “total” composition.

When comparing the primary axes of compositional variation, we found strong support for the SVH, as was also reported by Draper et al. (2019) for Amazonian tree communities ($r^2 = 0.85$). In contrast, Hakkenberg, Peet, et al. (2018), who included all vascular plants in the field-based community, found weaker support for the SVH in North American temperate forests (Spearman’s $r = 0.536$). Here, we defined the community as only canopy trees, potentially explaining the greater degree of association between spectral and field-based composition, as only the uppermost layer of vegetation is what was imaged. Aligned with this argument, we found that the primary axis of VNIR–spectral composition was more tightly associated with the primary axis of functional than taxonomic composition, as traits and not species identity drive reflectance patterns (Ustin & Gamon, 2010). The primary axes of VNIR–spectral, taxonomic, and functional composition were strongly associated and captured the turnover from temperate to boreal communities. In contrast, the primary axis of SWIR–spectral composition was not related to the primary axes of field-based composition. The difference in degree of

FIGURE 5 Effect of elevation meters above sea level (m asl) on (a) taxonomic (exponential Shannon’s Index; 1D), (b) functional (functional dispersion; F_{Dis}), and (c) visible to near-infrared (VNIR)–spectral (spectral variance; SV) diversity as modeled by general additive models (GAMs), where the smoothing parameter was estimated using restricted maximum likelihood (REML; $n = 50$). Smoothed function is the solid black line, gray shading denotes SE, and points are raw data.

association between the two spectral data sets may have arisen because we normalized the hyperspectral data using continuum removal (described below).

Using a multivariate approach, we found “total” spectral composition was moderately related to “total” field-based composition, which is consistent with a previous study in which plot-wise ordinations of mean spectral reflectance were related to ordinations of taxonomic composition across North American biomes (average covariance = 47%; Schweiger & Laliberté, 2022). Taking an alternative multivariate approach, Féret and Asner (2014) also demonstrated support for the SVH. They found a strong association between compositional dissimilarity matrices summarizing spectral composition and taxonomic composition of Amazonian tree communities (average Mantel’s $r = 0.68$). In contrast to the univariate approach, we found the magnitude of correspondence with the field-based dimensions to be similar regardless of whether spectral composition was composed of either VNIR or SWIR wavelengths. When it was composed of the VNIR wavelengths, the degree of “total” association was the result of the strong correspondence between the primary axes of compositional variation across the dimensions and weaker correspondence of the secondary axes of variation (Appendix S1: Figure S6). However, when it was composed of the SWIR wavelengths, the degree of “total” association was the result of the strong correspondence of the secondary axes of variation (Appendix S1: Figure S6). Given that secondary axes that explain relatively small proportions of variation can drive multivariate associations, we caution against using the strength of multivariate association alone to draw conclusions on the utility of spectral composition.

Effect of metric on spectral-field-based diversity relationship

Findings from a multisite study suggest that spectral diversity is most strongly associated with field-based diversity in forest ecosystems (Schweiger & Laliberté, 2022); however, the number of studies examining the SVH using fine spatial resolution hyperspectral data in forest ecosystems has been limited and findings have been mixed (for support see Carlson et al., 2007; Féret & Asner, 2014; in contrast, see Kamoske et al., 2022). We demonstrate that the choice of spectral and field-based diversity metrics affects the degree of association, where conclusions range from no support to strong support for the SVH, potentially explaining inconsistencies in the spectral-field-based diversity relationships. Going forward, it is important that conclusions regarding the efficacy of spectral diversity not be confounded by the

metrics used to measure it and/or the metrics used to measure field-based diversity. Additionally, differences in data acquisition could contribute to mixed support for the SVH, both in terms of field methodology and hyperspectral imaging (e.g., Rossi et al., 2021). We found that spectral diversity composed of VNIR wavelengths was more associated with field-based diversity than when spectral diversity was composed of SWIR wavelengths (discussed below). However, the effect of spectral and field-based metrics was similar with regard to the wavelengths that the spectral diversity was composed of.

For the taxonomic dimension, we found that spectral diversity was more closely associated with abundance-weighted diversity metrics than species richness, aligning with the findings of others (Gholizadeh et al., 2019; Oldeland et al., 2010; Schweiger & Laliberté, 2022; Wang, Gamon, Cavender-Bares, et al., 2018; Wang, Gamon, Schweiger, et al., 2018). The importance of incorporating information on species evenness when relating spectral diversity to taxonomic diversity is intuitive; assuming equal species richness, a community with low species evenness (e.g., one dominant species) should be less spectrally heterogeneous than a community with higher evenness. However, species evenness alone lacks information on species richness and, thus, information on how many different phenotypes with presumably different spectral signals are present. Therefore, assuming equal species evenness, a community with high richness should be more spectrally heterogeneous than a community with low richness (Wang, Gamon, Cavender-Bares, et al., 2018; Wang, Gamon, Schweiger, et al., 2018). Nonetheless, we found that spectral diversity was comparably related to species evenness (Pielou’s evenness index, J') as diversity metrics that integrate both species richness and evenness (exponential Shannon’s index and inverse Simpson’s index, 1D and 2D , respectively). We argue that this is driven by the positive relationship between species evenness and functional divergence in this system, where communities with high species evenness are composed of mixed forests that have high trait divergence between broadleaf deciduous and coniferous species and occupy large volumes of functional space (further discussed below). However, we do not expect this trend to hold more generally; for example, Wang, Gamon, Cavender-Bares, et al. (2018) found spectral diversity to be more strongly correlated with taxonomic diversity metrics that incorporated richness and evenness (Shannon’s index and Simpson’s index) than species evenness alone (J') in an experimental prairie ecosystem.

In agreement with our predictions, we found that the maximum degree of association between spectral and field-based diversity was greater for functional than taxonomic diversity (Ustin & Gamon, 2010). Moreover,

spectral diversity was more tightly associated with functional richness than species richness. However, like taxonomic diversity, the magnitude of association was dependent on the functional diversity metric to which spectral diversity was compared. We found spectral diversity was most strongly related to functional dispersion (F_{Dis}) and Rao's entropy (RaoQ), two closely related metrics that integrate functional richness and divergence and are weighted by species abundance (de Bello et al., 2021; Mason et al., 2013). Spectral diversity was moderately related to functional richness (F_{Ric}) but was not associated with functional divergence (F_{Div}). Functional richness, or the range of functional space occupied by a community, is solely based on extreme trait values and is independent of species abundances (Legras et al., 2018; Villéger et al., 2008), indicating that species with extreme trait values and, presumably, unique spectra strongly affect spectral diversity regardless of the abundance in which they occur. Unlike functional dispersion or Rao's entropy, functional divergence reflects the distribution of species abundance in functional space independent of functional richness, where functional divergence is high when the most abundant species are distributed on the margins of trait space (Villéger et al., 2008). While one might expect a community in which the most abundant species are functionally dissimilar (i.e., high F_{Div}) to be highly spectrally heterogeneous, our findings suggest that spectral diversity increases with functional dissimilarity between species only after accounting for the range of functional space occupied by the community. To the best of our knowledge, we are the first to examine the relationship between spectral diversity and the different elements of functional diversity. Future studies are needed to examine the generality of these trends.

Our results demonstrate that choice of spectral diversity metric affects the degree of correspondence between spectral and field-based diversity. Ideally, spectral diversity metrics reflect characteristics of the plant community and not values in the hyperspectral data that come from other sources, such as spectral noise, bare-ground reflectance (Gholizadeh et al., 2018), illumination geometry (Weyermann et al., 2014), and/or standing dead biomass (Rossi et al., 2021). Previous studies cautioned that spectral metrics that are heavily influenced by extreme values should be used with care (Gholizadeh et al., 2018; Rossi et al., 2021). However, we found that spectral metrics that are more influenced by extreme values (i.e., CHV and SV) were more associated with field-based diversity metrics, suggesting that here extreme spectral values contain information about the community. We speculate that this is because closed-canopy forests consisting of mature trees are less likely to have confounding factors (e.g., bare

ground) than ecosystems with more open canopies, such as grasslands (Schweiger & Laliberté, 2022). Additionally, we smoothed and normalized reflectance spectra potentially minimizing or removing extreme spectral values from other sources.

Environmental drivers of community properties

If variation in hyperspectral reflectance profiles is assumed to be an expression of variation in taxonomic and functional identity (Cavender-Bares et al., 2017; Kothari & Schweiger, 2022), one would expect spatial patterns in spectral community properties along environmental gradients to mirror changes in field-based community properties. Despite calls for a wider application of hyperspectral data (Cavender-Bares et al., 2017; Kothari & Schweiger, 2022), few studies have extended the SVH to assess the ability to examine ecological processes via spectral community properties (but see Schweiger et al., 2018; Wallis et al., 2023; Williams et al., 2021). The same qualitative conclusions about the environmental drivers of canopy tree community properties at Mont Mégantic arose when modeled using either spectral or field-based community properties. However, this was only the case when spectral properties were quantified using VNIR but not SWIR wavelengths. This aligns with our findings from the degree-of-correspondence analyses, as spectral properties quantified using VNIR wavelengths were more strongly related to field-based properties. The extent to which spectral community properties can be applied to examine ecological phenomena is dependent on sufficiently tight associations with field-based community properties. The observed spatial patterns in taxonomic, functional, and VNIR-spectral composition and diversity were strongly related to the temperate-to-boreal gradient.

The transition from temperate to boreal communities along eastern North American mountainsides is visually striking, and, unsurprisingly, elevation explained the majority of fitted variation in taxonomic and functional composition, a conclusion also derived from modeling VNIR-spectral composition. While climate plays a key role in driving composition change along elevation gradients (Cogbill & White, 1991; Foster & D'Amato, 2015), other environmental factors, particularly soil properties, that covary with elevation also influence the turnover from temperate to boreal communities (Carteron et al., 2020). When these additional environmental factors do not covary with broad climate gradients, they can result in fine-scale heterogeneity in species composition (Goldblum & Rigg, 2010). For example, we found that slope affected taxonomic

and functional composition: At low elevation, slope separated deciduous from mixed forest communities—again, a conclusion also derived from modeling VNIR-spectral composition. This pattern is attributed to cold-air pooling, where downslope drainage of cold air results in lower temperatures in low-lying depressions and valleys (i.e., flatter slopes) and selects for increased coniferous cover, both boreal and temperate conifer species, compared to surrounding temperate communities (Cogbill & White, 1991; Goldblum & Rigg, 2010; Pastore et al., 2022). Moreover, we found that aspect (i.e., northness) affected taxonomic and functional composition, driven by mid-elevation plots characterized by mixed forest communities with a relatively high abundance of red spruce and high CWM of lignin concentration. More northern-facing slopes presumably are characterized by colder conditions that select for increased abundance of boreal species (Cogbill & White, 1991), but contrasting patterns have also been demonstrated (Foster & D'Amato, 2015). Nevertheless, the effect of aspect observed here might be an artifact of plot distribution as most mid-elevation plots, where red spruce is generally most abundant (Marcotte & Grandtner, 1974), were established on more northern-facing slopes (Appendix S1: Figure S8). Regardless, unlike elevation and slope, aspect did not affect VNIR-spectral composition, suggesting that spectral composition is limited to detecting broad compositional changes (i.e., temperate-to-boreal turnover) and not finer changes associated with variation in the abundance of individual species.

Elevation also explained the vast majority of fitted variation in taxonomic, functional, and VNIR-spectral diversity. We observed a multimodal pattern, where taxonomic and functional diversity was greatest at low-elevation plots located along the valley bottom and at mid-elevation plots, a conclusion also derived by modeling VNIR-spectral diversity relationships. Similar relationships between diversity metrics should not be surprising since they represent aspects of the same phenomenon (Morris et al., 2014). Here, communities with the greatest diversity are mixed forest communities, composed of both broadleaved temperate and coniferous boreal species that occupy different ends of the foliar trait continuum (i.e., high trait divergence). Ecotonal communities like these are often considered to have higher diversity, potentially driven by relaxed constraints on co-existence (He et al., 2023). Additionally, functional diversity increased with the degree of northness, driven by mid-elevation mixed forest communities. In contrast, aspect did not affect taxonomic diversity because the mixed forest communities at low elevations were more diverse than those at mid-elevations due to increased species richness. In line with theory and findings from degree-of-correspondence analyses, conclusions drawn from modeling VNIR-spectral diversity mirrored

functional diversity, and not taxonomic diversity, where VNIR-spectral diversity increased with the degree of northness. As with the effect of aspect on composition, we argue that the effect on functional and VNIR-spectral diversity is a spurious result driven by plot distribution (Appendix S1: Figure S8).

Importance of wavelengths

Field-based community properties were strongly related to the turnover from broadleaved, deciduous temperate forests to coniferous boreal forests. Functionally, broadleaf, deciduous angiosperms and evergreen conifers occupy opposite positions along a continuum of foliar traits, with coniferous species characterized by relatively low N content, specific leaf area (SLA), and photosynthetic activity (Díaz et al., 2016; Reich, 2014). Beyond foliar traits, which composed the functional dimension here, these clades also differ in crown architecture, with deciduous angiosperms characterized by decurrent growth and ellipsoidal crowns, as opposed to coniferous species that are characterized by excurrent growth and canonical crowns (Brown et al., 1967; Walker & Kenkel, 2000). Spectrally, the NIR-SWIR region (specifically, 750–1400 nm) is generally considered important for distinguishing these two clades, with canopy reflectance generally lower for coniferous canopies than broadleaf, deciduous canopies (Hovi et al., 2018; Ollinger, 2011; Williams, 1991). At the community level, whole-canopy reflectance profiles (i.e., spectral composition) represent the integrated effects of foliar and crown traits and is influenced by multiple species (Ollinger, 2011). Not only are foliar traits of evergreen needles causally and correlatively associated with lower NIR-SWIR reflectance compared to deciduous broadleaves (Jacquemoud & Ustin, 2019; Ollinger, 2011), but coniferous crown architecture is also associated with lower NIR-SWIR reflectance (Rautiainen & Stenberg, 2005; Smolander & Stenberg, 2003). Nevertheless, we found that mean normalized reflectance in the visible region captured the turnover in composition from broadleaf, deciduous communities to coniferous communities (i.e., the primary axis of VNIR-spectral composition; Figure 2d). Moreover, the visible region most strongly contributed to spectral diversity as quantified by SV, where mixed forest plots had the greatest within-plot variance in the normalized reflectance in the visible region (Appendix S1: Figure S4). We argue that the importance of the visible region is likely due to the fact that we normalized the hyperspectral data using continuum removal.

Continuum removal is a brightness normalization technique that can address illumination differences that

may remain in imagery after standard processing procedures and could introduce spurious spectral variation (Serbin & Townsend, 2020). This procedure emphasizes differences in absorption features and suppresses variation in overall brightness among spectra (Clark & Roush, 1984), reducing the effects of changing illumination conditions among and between flightlines but also reducing canopy structural effects (Serbin & Townsend, 2020). Given that pigments show strong absorption features in the visible region (Jacquemoud & Baret, 1990; Ustin et al., 2009) and that pigment content differs between broadleaf deciduous and coniferous species (Li et al., 2018), it is unsurprising that we found a tighter degree of association with field-based communities properties with spectral community properties composed of VNIR wavelengths. While other biochemicals have known, albeit weak, absorption features in the SWIR and differ between the two clades (e.g., cellulose and lignin content), these absorption features are often overlapping (Curran, 1989), which might explain why the degree of association between spectral and field-based community properties was weaker when they were composed of SWIR wavelengths. The predictive capacity of spectral community properties will likely depend on the wavelengths of which they are composed (Appendix S1: Section S2; Imran et al., 2021); however, the importance of wavelengths will likely depend on methodological choices surrounding spectral transformation techniques (Aneece et al., 2017). In addition to the wavelengths sampled, the two hyperspectral data sets here also differ in other properties that might contribute to the SWIR–spectral community properties being less strongly associated with field-based community properties. The SWIR–spectral data have a lower spatial and spectral resolution; however, they cover a larger spectral range.

CONCLUSIONS

The simplicity of the SVH makes spectral community properties an intriguing approach for quantifying plant biodiversity from hyperspectral data, especially because they can be quantified directly from imagery without a priori field knowledge. Choosing the method or metric used to quantify community properties, both field-based and spectral, is an important methodological step. We demonstrate that these methodological decisions affect conclusions regarding the utility of the spectral community property approach. To move toward a consensus on what methods and metrics perform best, it is critical that additional studies examine the relationships between the various ways to quantify spectral and field-based community properties. A particular focus should be placed on

properties that go beyond taxonomic diversity, as the SVH has most commonly been examined using taxonomic diversity metrics. Comparing results across studies may be complicated by additional factors that can influence the degree of association between spectral and field-based community properties, including factors associated with field and spectral data acquisition, spectral transformation techniques and wavelength regions used, and ecosystem specific properties (i.e., plant size, abundance, and timing of nonphotosynthetic materials).

While imaging spectrometers are usually presented as important instruments for monitoring plant biodiversity, we show that spectral community properties have the potential to further our understanding on the distribution of community properties across space. Using spectral community properties can help overcome methodological limitations of field-based studies, such as relatively small sample sizes, limited spatial coverage, and lack of in situ trait measurements. However, using spectral community properties is not without challenges as we currently do not understand all the phenotypic variation that drive spectra, some of which may not be important for plant fitness or function (Kothari & Schweiger, 2022). Understanding how spectral community properties relate to field-based community properties is a crucial first step—if they are not sufficiently associated, ecological conclusions derived from spectral community properties might not align with those derived using field-based community properties. Future multisite studies are needed to examine the generality of the spectral variation hypothesis across temperate and boreal forest ecosystems. We would recommend that these studies, and studies in general examining the SVH, be conducted in such a way as to carefully consider the method or metric used to quantify community properties. We recognize that plant phenological changes and other temporal differences (e.g., drought stress, mast years) can result in large temporal variation in hyperspectral reflectance and, thus, influence the link between spectral and field-based community properties (Fassnacht et al., 2022). Our findings are limited to peak growing season, a timing that aligns with standardized foliar functional trait protocols (Pérez-Harguindeguy et al., 2013) and that will be most practical to replicate in other surveys, including resurveys of the same sites. With these caveats in mind, future studies could use spatial patterns in spectral composition and diversity to test hypotheses on community assembly processes or elucidate drivers of ecosystem function across broad gradients spanning temperate to boreal ecosystems.

AUTHOR CONTRIBUTIONS

Anna L. Crofts and Mark Vellend designed the study with contributions from Etienne Laliberté. Anna

L. Crofts and Sabine St-Jean conducted the forest inventory surveys. Sabrina Demers-Thibeault led the leaf sampling and foliar trait quantification with contributions from Anna L. Crofts and Etienne Laliberté. Deep Inamdar, J. Pablo Arroyo-Mora, and Margaret Kalacska acquired and preprocessed the aerial hyperspectral data and Christine I. B. Wallis postprocessed the aerial hyperspectral data. Anna L. Crofts analyzed the data, interpreted the results, and wrote the first draft, with substantial contributions from Mark Vellend. All authors contributed to further revisions of the paper.

ACKNOWLEDGMENTS

This study was conducted within the framework of the Canadian Airborne Biodiversity Observatory (CABO) project. We would like to thank the CABO members and the many field and laboratory assistants who contributed to the forest inventory surveys, leaf sampling and foliar trait quantification, and imaging spectroscopy. Additionally, we thank Raymond Soffer from the National Research Council Canada for his help with the preprocessing of the hyperspectral data. We thank the Société des établissements de plein air du Québec, particularly the staff of Parcs nationaux des Mont-Mégantic and Mont-Saint-Bruno, who provided access to the field sites and ongoing support for our research. CABO was funded by a Discovery Frontiers grant from the Natural Sciences and Engineering Research Council of Canada (NSERC, 509190-2017). Additional financial support by student scholarships provided by NSERC (53495-2019) and the Royal Canadian Geographic Society.

CONFLICT OF INTEREST STATEMENT

The authors declare no conflicts of interest.

DATA AVAILABILITY STATEMENT

Data (Crofts et al., 2024) are available in Dryad at <https://doi.org/10.5061/dryad.5mkkwh7dh>. These data are also publicly available in the Ecological Spectral Information System (EcoSIS) repository at <https://ecosis.org/package/cabo-canopy-level-spectra-from-forest-sites>. Code (Crofts, 2024) is publicly available in Zenodo at <https://doi.org/10.5281/zenodo.10735410>.

ORCID

Anna L. Crofts  <https://orcid.org/0000-0002-0098-1844>


Christine I. B. Wallis  <https://orcid.org/0000-0002-0794-3146>

Sabine St-Jean  <https://orcid.org/0009-0008-3851-824X>

Deep Inamdar  <https://orcid.org/0000-0002-7810-7356>

J. Pablo Arroyo-Mora  <https://orcid.org/0000-0003-0287-8960>

Margaret Kalacska  <https://orcid.org/0000-0002-1676-481X>

Etienne Laliberté  <https://orcid.org/0000-0002-3167-2622>

Mark Vellend  <https://orcid.org/0000-0002-2491-956X>

REFERENCES

- Anderson, D. R., K. P. Burnham, W. R. Gould, and S. Cherry. 2001. "Concerns about Finding Effects that Are Actually Spurious." *Wildlife Society Bulletin* 29: 311–16.
- Aneece, I. P., H. Epstein, and M. Lerda. 2017. "Correlating Species and Spectral Diversities Using Hyperspectral Remote Sensing in Early-Successional Fields." *Ecology and Evolution* 7: 3475–88.
- Botta-Dukát, Z. 2005. "Rao's Quadratic Entropy as a Measure of Functional Diversity Based on Multiple Traits." *Journal of Vegetation Science* 16: 533–540.
- Brown, C. L., R. G. McAlpine, and P. P. Kormanik. 1967. "Apical Dominance and Form in Woody Plants: A Reappraisal." *American Journal of Botany* 54: 153.
- Carlson, K. M., G. P. Asner, R. F. Hughes, R. Ostertag, and R. E. Martin. 2007. "Hyperspectral Remote Sensing of Canopy Biodiversity in Hawaiian Lowland Rainforests." *Ecosystems* 10: 536–549.
- Carteron, A., V. Parasquive, F. Blanchard, X. Guilbeault-Mayers, B. L. Turner, M. Vellend, and E. Laliberté. 2020. "Soil Abiotic and Biotic Properties Constrain the Establishment of a Dominant Temperate Tree into Boreal Forests." *Journal of Ecology* 108: 931–944.
- Cavender-Bares, J., J. A. Gamon, S. E. Hobbie, M. D. Madritch, J. E. Meireles, A. K. Schweiger, and P. A. Townsend. 2017. "Harnessing Plant Spectra to Integrate the Biodiversity Sciences across Biological and Spatial Scales." *American Journal of Botany* 104: 966–69.
- Clark, R. N., and T. L. Roush. 1984. "Reflectance Spectroscopy: Quantitative Analysis Techniques for Remote Sensing Applications." *Journal of Geophysical Research: Solid Earth* 89: 6329–40.
- Cogbill, C. V., and P. S. White. 1991. "The Latitude-Elevation Relationship for Spruce-Fir Forest and Treeline along the Appalachian Mountain Chain." *Vegetatio* 94: 153–175.
- Crofts, A. L. 2024. "ALCrofts/CABO_SVH_Forest_Sites: CABO_SVH_Forests (v1.0)." Zenodo. <https://doi.org/10.5281/zenodo.10735410>.
- Crofts, A. L., S. St-Jean, and M. Vellend. 2022. "Canadian Airborne Biodiversity Observatory's Forest Inventory Field Survey Protocol V.2." protocols.io. <https://doi.org/10.17504/protocols.io.q26g7rn23vwz/v2>.
- Crofts, A. L., C. I. B. Wallis, S. St-Jean, S. Demers-Thibeault, D. Inamdar, J. P. Arroyo-Mora, M. Kalacska, E. Laliberté, and M. Vellend. 2024. "CABO Forest Inventory Survey Data: Canopy-Level Spectra, Species Abundances, and Environmental Conditions." Dryad, Dataset. <https://doi.org/10.5061/dryad.5mkkwh7dh>.
- Curran, P. J. 1989. "Remote Sensing of Foliar Chemistry." *Remote Sensing of Environment* 30: 271–78.
- Dahlin, K. M. 2016. "Spectral Diversity Area Relationships for Assessing Biodiversity in a Wildland-Agriculture Matrix." *Ecological Applications* 26: 2756–66.
- Daly, A. J., J. M. Baetens, and B. De Baets. 2018. "Ecological Diversity: Measuring the Unmeasurable." *Mathematics* 6: 119.
- de Bello, F., Z. Botta-Dukát, J. Lepš, and P. Fibich. 2021. "Towards a more Balanced Combination of Multiple Traits when

- Computing Functional Differences between Species.” *Methods in Ecology and Evolution* 12: 443–48.
- Díaz, S., J. Kattge, J. H. C. Cornelissen, I. J. Wright, S. Lavorel, S. Dray, B. Reu, et al. 2016. “The Global Spectrum of Plant Form and Function.” *Nature* 529: 167–171.
- Draper, F. C., C. Baraloto, P. G. Brodrick, O. L. Phillips, R. V. Martinez, E. N. Honorio Coronado, T. R. Baker, et al. 2019. “Imaging Spectroscopy Predicts Variable Distance Decay across Contrasting Amazonian Tree Communities.” *Journal of Ecology* 107: 696–710.
- Fassnacht, F. E., J. Müllerová, L. Conti, M. Malavasi, and S. Schmidtlein. 2022. “About the Link between Biodiversity and Spectral Variation.” *Applied Vegetation Science* 25: e12643.
- Féret, J. B., and G. P. Asner. 2014. “Mapping Tropical Forest Canopy Diversity Using High-Fidelity Imaging Spectroscopy.” *Ecological Applications* 24: 1289–96.
- Foster, J. R., and A. W. D’Amato. 2015. “Montane Forest Ecotones Moved Downslope in Northeastern USA in Spite of Warming between 1984 and 2011.” *Global Change Biology* 21: 4497–4507.
- Frye, H. A., M. E. Aiello-Lammens, D. Euston-Brown, C. S. Jones, H. Kilroy Mollmann, C. Merow, J. A. Slingsby, H. van der Merwe, A. M. Wilson, and J. A. Silander. 2021. “Plant Spectral Diversity as a Surrogate for Species, Functional and Phylogenetic Diversity across a Hyper-Diverse Biogeographic Region.” *Global Ecology and Biogeography* 30: 1403–17.
- Funk, J. L., J. E. Larson, G. M. Ames, B. J. Butterfield, J. Cavender-Bares, J. Firn, D. C. Laughlin, A. E. Sutton-Grier, L. Williams, and J. Wright. 2017. “Revisiting the Holy Grail: Using Plant Functional Traits to Understand Ecological Processes.” *Biological Reviews* 92: 1156–73.
- Gholizadeh, H., J. A. Gamon, P. A. Townsend, A. I. Zyguelbaum, C. J. Helzer, G. Y. Hmimina, R. Yu, R. M. Moore, A. K. Schweiger, and J. Cavender-Bares. 2019. “Detecting Prairie Biodiversity with Airborne Remote Sensing.” *Remote Sensing of Environment* 221: 38–49.
- Gholizadeh, H., J. A. Gamon, A. I. Zyguelbaum, R. Wang, A. K. Schweiger, and J. Cavender-Bares. 2018. “Remote Sensing of Biodiversity: Soil Correction and Data Dimension Reduction Methods Improve Assessment of α -Diversity (Species Richness) in Prairie Ecosystems.” *Remote Sensing of Environment* 206: 240–253.
- Goldblum, D., and L. S. Rigg. 2010. “The Deciduous Forest—Boreal Forest Ecotone.” *Geography Compass* 4: 701–717.
- Grime, J. P. 1979. *Plant Strategies and Vegetation Processes*. Chichester: John Wiley & Sons.
- Hakkenberg, C. R., R. K. Peet, D. L. Urban, and C. Song. 2018. “Modeling Plant Composition as Community Continuum in a Forest Landscape with LiDAR and Hyperspectral Remote Sensing.” *Ecological Applications* 28: 177–190.
- Hakkenberg, C. R., K. Zhu, R. K. Peet, and C. Song. 2018. “Mapping Multi-Scale Vascular Plant Richness in a Forest Landscape with Integrated LiDAR and Hyperspectral Remote-Sensing.” *Ecology* 99: 474–487.
- He, P., S. Fontana, C. Ma, H. Liu, L. Xu, R. Wang, Y. Jiang, and M. H. Li. 2023. “Using Leaf Traits to Explain Species Co-existence and its Consequences for Primary Productivity across a Forest-Steppe Ecotone.” *Science of the Total Environment* 859: 160139.
- Hijmans, R. J. 2023. “terra: Spatial Data Analysis.” R Package Version 1.7-3. <https://CRAN.R-project.org/package=terra>.
- Hill, M. O. 1973. “Diversity and Evenness: A Unifying Notation and its Consequences.” *Ecology* 54: 427–432.
- Hovi, A., P. Forsström, M. Mõttus, and M. Rautiainen. 2018. “Evaluation of Accuracy and Practical Applicability of Methods for Measuring Leaf Reflectance and Transmittance Spectra.” *Remote Sensing* 10: 25.
- Imran, H. A., D. Gianelle, M. Scotton, D. Rocchini, M. Dalponte, S. Macolino, K. Sakowska, C. Pornaro, and L. Vescovo. 2021. “Potential and Limitations of Grassland α -Diversity Prediction Using Fine-Scale Hyperspectral Imagery.” *Remote Sensing* 13: 2649.
- Inamdar, D., M. Kalacska, J. P. Arroyo-Mora, and G. Leblanc. 2021. “The Directly-Georeferenced Hyperspectral Point Cloud: Preserving the Integrity of Hyperspectral Imaging Data.” *Frontiers in Remote Sensing* 2: 675323.
- Inamdar, D., M. Kalacska, P. Osei Darko, J. P. Arroyo-Mora, and G. Leblanc. 2023. “Spatial Response Resampling (SR²): Accounting for the Spatial Point Spread Function in Hyperspectral Image Resampling.” *MethodsX* 10: 101998.
- Jacquemoud, S., and F. Baret. 1990. “PROSPECT: A Model of Leaf Optical Properties Spectra.” *Remote Sensing of Environment* 34: 75–91.
- Jacquemoud, S., and S. Ustin. 2019. *Leaf Optical Properties*. Cambridge: Cambridge University Press.
- Kamoske, A. G., K. M. Dahlin, Q. D. Read, S. Record, S. C. Stark, S. P. Serbin, P. L. Zarnetske, and M. Dornelas. 2022. “Towards Mapping Biodiversity from above: Can Fusing Lidar and Hyperspectral Remote Sensing Predict Taxonomic, Functional, and Phylogenetic Tree Diversity in Temperate Forests?” *Global Ecology and Biogeography* 31: 1440–60.
- Kattge, J., G. Bönisch, S. Díaz, S. Lavorel, I. C. Prentice, P. Leadley, S. Tautenhahn, et al. 2020. “TRY Plant Trait Database—Enhanced Coverage and Open Access.” *Global Change Biology* 26: 119–188.
- Kothari, S., R. Beauchamp-Rioux, F. Blanchard, A. L. Crofts, A. Girard, X. Guilbeault-Mayers, P. W. Hacker, et al. 2023. “Predicting Leaf Traits across Functional Groups Using Reflectance Spectroscopy 1.2.” *New Phytologist* 2338: 549–566.
- Kothari, S., and A. K. Schweiger. 2022. “Plant Spectra as Integrative Measures of Plant Phenotypes.” *Journal of Ecology* 110: 2536–54.
- Laliberté, E., and P. Legendre. 2010. “A Distance-Based Framework for Measuring Functional Diversity from Multiple Traits.” *Ecology* 91: 299–305.
- Laliberté, E., P. Legendre, and B. Shipley. 2014. “FD: Measuring Functional Diversity from Multiple Traits, and Other Tools for Functional Ecology.” R Package Version 1.0-12.1. <https://CRAN.R-project.org/package=FD>.
- Laliberté, E., A. K. Schweiger, and P. Legendre. 2020. “Partitioning Plant Spectral Diversity into Alpha and Beta Components.” *Ecology Letters* 23: 370–380.
- Larsen, K. 2015. “GAM: The Predictive Modeling Silver Bullet.” Multithreaded, Stich Fix. <https://multithreaded.stitchfix.com/blog/2015/07/30/gam/>.
- Lavorel, S., and E. Garnier. 2002. “Predicting Changes in Community Composition and Ecosystem Functioning from Plant Traits: Revisiting the Holy Grail.” *Functional Ecology* 16: 545–556.

- Leboeuf, A., I. Pomerleau, S. Vézeau, and S. Lacroix. 2015. *Province-Wide LiDAR Data Acquisition: Impact Analysis and Recommendations*. Québec: Ministère des Forêts, de la Faune et des Parcs (MFFP) du Québec, Gouvernement du Québec.
- Legendre, P., and L. Legendre. 2012. *Numerical Ecology*, 3rd ed. Amsterdam: Elsevier.
- Legendre, P., J. Oksanen, and C. J. ter Braak. 2011. "Testing the Significance of Canonical Axes in Redundancy Analysis." *Methods in Ecology and Evolution* 2: 269–277.
- Legras, G., N. Loiseau, and J. C. Gaertner. 2018. "Functional Richness: Overview of Indices and Underlying Concepts." *Acta Oecologica* 87: 34–44.
- Lehnert, L. W., H. Meyer, W. A. Obermeier, B. Silva, B. Regeling, B. Thies, and J. Bendix. 2019. "Hyperspectral Data Analysis in R: The hsdar Package." *Journal of Statistical Software* 89: 1–23.
- Li, D. 2018. "hillR: Taxonomic, Functional, and Phylogenetic Diversity and Similarity through Hill Numbers." *Journal of Open Source Software* 3: 1041.
- Li, Y., N. He, J. Hou, L. Xu, C. Liu, J. Zhang, Q. Wang, X. Zhang, and X. Wu. 2018. "Factors Influencing Leaf Chlorophyll Content in Natural Forests at the Biome Scale." *Frontiers in Ecology and Evolution* 6: 64.
- MacArthur, R. H. 1965. "Patterns of Species Diversity." *Biological Reviews* 40: 510–533.
- Magurran, A., and B. McGill. 2010. *Biological Diversity: Frontiers in Measurements and Assessment*. Oxford: Oxford University Press.
- Marcotte, G., and M. M. Grandtner. 1974. "Étude écologique de la végétation forestière du Mont Mégantic." Service de la recherche, Direction général des forêts, Ministère des terres et forêts, Québec.
- Mason, N. W. H., F. De Bello, D. Mouillot, S. Pavoine, and S. Dray. 2013. "A Guide for Using Functional Diversity Indices to Reveal Changes in Assembly Processes along Ecological Gradients." *Journal of Vegetation Science* 24: 794–806.
- McGill, B. J., B. J. Enquist, E. Weiher, and M. Westoby. 2006. "Rebuilding Community Ecology from Functional Traits." *Trends in Ecology & Evolution* 21: 178–185.
- Morris, E. K., T. Caruso, F. Buscot, M. Fischer, C. Hancock, T. S. Maier, T. Meiners, et al. 2014. "Choosing and Using Diversity Indices: Insights for Ecological Applications from the German Biodiversity Exploratories." *Ecology and Evolution* 4: 3514–24.
- Natural Resources Canada (NRCAN). 2008. *Canada's National Forest Inventory Ground Sampling Guidelines: Specifications for Ongoing Measurements, Ver. 5.0*. Victoria: Canadian Forest Service, Pacific Forestry Centre.
- Oksanen, J., G. L. Simpson, F. G. Blanchet, R. Kindt, P. Legendre, P. R. Minchin, R. B. O'Hara, et al. 2022. "vegan: Community Ecology Package." R Package Version 2.6-4. <https://CRAN.R-project.org/package=vegan>.
- Oldeland, J., D. Wesuls, D. Rocchini, M. Schmidt, and N. Jürgens. 2010. "Does Using Species Abundance Data Improve Estimates of Species Diversity from Remotely Sensed Spectral Heterogeneity?" *Ecological Indicators* 10: 390–96.
- Ollinger, S. V. 2011. "Sources of Variability in Canopy Reflectance and the Convergent Properties of Plants." *New Phytologist* 189: 375–394.
- Palmer, M. W., P. G. Earls, B. W. Hoagland, P. S. White, and T. Wohlgemuth. 2002. "Quantitative Tools for Perfecting Species Lists." *Environmetrics* 13: 121–137.
- Pastore, M. A., A. T. Classen, A. W. D'Amato, J. R. Foster, and E. C. Adair. 2022. "Cold-Air Pools as Microrefugia for Ecosystem Functions in the Face of Climate Change." *Ecology* 103: e3717.
- Pérez-Harguindeguy, N., S. Díaz, E. Garnier, P. Jaureguilberry, L. Poorter, H. ter Steege, and J. H. C. Cornelissen. 2013. "New Handbook for Standardized Measurement of Plant Functional Traits Worldwide." *Australian Journal of Botany* 61: 167–234.
- Pielou, E. 1966. "The Measurement of Diversity in Different Types of Biological Collections." *Journal of Theoretical Biology* 13: 131–144.
- Purvis, A., and A. Hector. 2000. "Getting the Measure of Biodiversity." *Nature* 405: 212–19.
- R Core Team. 2021. *R: A Language and Environment for Statistical Computing*. Vienna: R Foundation for Statistical Computing.
- Rautiainen, M., and P. Stenberg. 2005. "Application of Photon Recollision Probability in Coniferous Canopy Reflectance Simulations." *Remote Sensing of Environment* 96: 98–107.
- Reich, P. B. 2014. "The World-Wide "Fast-Slow" Plant Economics Spectrum: A Traits Manifesto." *Journal of Ecology* 102: 275–301.
- Richter, R., and D. Schläpfer. 2020. "ATCOR-4 User Guide." In *Atmospheric/Topographic Correction for Airborne Imagery*. Wessling: DRL–German Aerospace Center.
- Rocchini, D., N. Balkenhol, G. A. Carter, G. M. Foody, T. W. Gillespie, K. S. He, S. Kark, et al. 2010. "Remotely Sensed Spectral Heterogeneity as a Proxy of Species Diversity: Recent Advances and Open Challenges." *Ecological Informatics* 5: 318–329.
- Rocchini, D., S. Luque, N. Pettorelli, L. Bastin, D. Doktor, N. Faedi, H. Feilhauer, et al. 2018. "Measuring β -Diversity by Remote Sensing: A Challenge for Biodiversity Monitoring." *Methods in Ecology and Evolution* 9: 1787–98.
- Rossi, C., M. Kneubühler, M. Schütz, M. E. Schaepman, R. M. Haller, and A. C. Risch. 2021. "Spatial Resolution, Spectral Metrics and Biomass Are Key Aspects in Estimating Plant Species Richness from Spectral Diversity in Species-Rich Grasslands." *Remote Sensing in Ecology and Conservation* 8: 297–314.
- Schmidtlein, S., and F. E. Fassnacht. 2017. "The Spectral Variability Hypothesis Does Not Hold across Landscapes." *Remote Sensing of Environment* 192: 114–125.
- Schweiger, A. K., J. Cavender-Bares, P. A. Townsend, S. E. Hobbie, M. D. Madritch, R. Wang, D. Tilman, and J. A. Gamon. 2018. "Plant Spectral Diversity Integrates Functional and Phylogenetic Components of Biodiversity and Predicts Ecosystem Function." *Nature Ecology and Evolution* 2: 976–982.
- Schweiger, A. K., and E. Laliberté. 2022. "Plant Beta-Diversity across Biomes Captured by Imaging Spectroscopy." *Nature Communications* 13: 2767.
- Serbin, S. P., and P. A. Townsend. 2020. "Scaling Functional Traits from Leaves to Canopies." In *Remote Sensing of Plant Biodiversity*, edited by J. Cavender-Bares, J. A. Gamon, and P. A. Townsend. Cham: Springer International Publishing.

- Shipley, B. 2010. *From Plant Traits to Vegetation Structure: Chance and Selection in the Assembly of Ecological Communities*. Cambridge: Cambridge University Press.
- Smolander, S., and P. Stenberg. 2003. "A Method to Account for Shoot Scale Clumping in Coniferous Canopy Reflectance Models." *Remote Sensing of Environment* 88: 363–373.
- Soffer, R. J., G. Ifimov, J. P. Arroyo-Mora, and M. Kalacska. 2019. "Validation of Airborne Hyperspectral Imagery from Laboratory Panel Characterization to Image Quality Assessment: Implications for an Arctic Peatland Surrogate Simulation Site." *Canadian Journal of Remote Sensing* 45: 476–508.
- Turner, W. 2014. "Sensing Biodiversity." *Science* 346: 301–2.
- Ustin, S. L., and J. A. Gamon. 2010. "Remote Sensing of Plant Functional Types." *New Phytologist* 186: 795–816.
- Ustin, S. L., A. A. Gitelson, S. Jacquemoud, M. Schaepman, G. P. Asner, J. A. Gamon, and P. Zarco-Tejada. 2009. "Retrieval of Foliar Information about Plant Pigment Systems from High Resolution Spectroscopy." *Remote Sensing of Environment* 113: S67–S77.
- van der Plas, F., T. Schröder-Georgi, A. Weigelt, K. Barry, S. Meyer, A. Alzate, R. L. Barnard, et al. 2020. "Plant Traits Alone Are Poor Predictors of Ecosystem Properties and Long-Term Ecosystem Functioning." *Nature Ecology and Evolution* 4: 1602–11.
- Villéger, S., N. W. H. Mason, and D. Mouillot. 2008. "New Multidimensional Functional Diversity Indices for a Multifaceted Framework in Functional Ecology." *Ecology* 89: 2290–2301.
- Walker, D. J., and N. C. Kenkel. 2000. "The Adaptive Geometry of Boreal Conifers." *Community Ecology* 1: 13–23.
- Wallis, C. I. B., A. L. Crofts, D. Inamdar, J. P. Arroyo-Mora, M. Kalacska, É. Laliberté, and M. Vellend. 2023. "Remotely Sensed Carbon Content: The Role of Tree Composition and Tree Diversity." *Remote Sensing of Environment* 284: 113333.
- Wang, R., and J. A. Gamon. 2019. "Remote Sensing of Terrestrial Plant Biodiversity." *Remote Sensing of Environment* 231: 111218.
- Wang, R., J. A. Gamon, J. Cavender-Bares, P. A. Townsend, and A. I. Zyguelbaum. 2018. "The Spatial Sensitivity of the Spectral Diversity-Biodiversity Relationship: An Experimental Test in a Prairie Grassland." *Ecological Applications* 28: 541–556.
- Wang, R., J. A. Gamon, C. A. Emmerton, H. Li, E. Nestola, G. Z. Pastorello, and O. Menzer. 2016. "Integrated Analysis of Productivity and Biodiversity in a Southern Alberta Prairie." *Remote Sensing* 8: 214.
- Wang, R., J. A. Gamon, A. K. Schweiger, J. Cavender-Bares, P. A. Townsend, A. I. Zyguelbaum, and S. Kothari. 2018. "Influence of Species Richness, Evenness, and Composition on Optical Diversity: A Simulation Study." *Remote Sensing of Environment* 211: 218–228.
- Westoby, M., D. S. Falster, A. T. Moles, P. A. Vesk, and I. J. Wright. 2002. "Plant Ecological Strategies: Some Leading Dimensions of Variation between Species." *Annual Review of Ecology and Systematics* 33: 125–159.
- Weyermann, J., A. Damm, M. Kneubuhler, and M. E. Schaepman. 2014. "Correction of Reflectance Anisotropy Effects of Vegetation on Airborne Spectroscopy Data and Derived Products." *IEEE Transactions on Geoscience and Remote Sensing* 52: 616–627.
- Williams, D. L. 1991. "A Comparison of Spectral Reflectance Properties at the Needle, Branch, and Canopy Level for Selected Conifer Species." *Remote Sensing of Environment* 35: 79–93.
- Williams, L. J., J. Cavender-Bares, P. A. Townsend, J. J. Couture, Z. Wang, A. Stefanski, C. Messier, and P. B. Reich. 2021. "Remote Spectral Detection of Biodiversity Effects on Forest Biomass." *Nature Ecology and Evolution* 5: 46–54.
- Wilson, M. F. J., B. O'Connell, C. Brown, J. C. Guinan, and A. J. Grehan. 2007. "Multiscale Terrain Analysis of Multibeam Bathymetry Data for Habitat Mapping on the Continental Slope." *Marine Geodesy* 30: 3–35.
- Wood, S. N. 2011. "Fast Stable Restricted Maximum Likelihood and Marginal Likelihood Estimation of Semiparametric Generalized Linear Models." *Journal of the Royal Statistical Society (B)* 73: 3–36.
- Zhu, L., B. Fu, H. Zhu, C. Wang, L. Jiao, and J. Zhou. 2017. "Trait Choice Profoundly Affected the Ecological Conclusions Drawn from Functional Diversity Measures." *Scientific Reports* 7: 3643.

SUPPORTING INFORMATION

Additional supporting information can be found online in the Supporting Information section at the end of this article.

How to cite this article: Crofts, Anna L., Christine I. B. Wallis, Sabine St-Jean, Sabrina Demers-Thibeault, Deep Inamdar, J. Pablo Arroyo-Mora, Margaret Kalacska, Etienne Laliberté, and Mark Vellend. 2024. "Linking Aerial Hyperspectral Data to Canopy Tree Biodiversity: An Examination of the Spectral Variation Hypothesis." *Ecological Monographs* e1605. <https://doi.org/10.1002/ecm.1605>